

Heavy meson semileptonic differential decay rate in two dimensions in the large N_c

Jorge Mondéjar, Antonio Pineda* and Joan Rojo

*Dept. d'Estructura i Constituents de la Matèria, U. Barcelona,
Diagonal 647, E-08028 Barcelona, Spain*

Abstract

We study QCD in 1+1 dimensions in the large N_c limit using light-front Hamiltonian perturbation theory in the $1/N_c$ expansion. We use this formalism to exactly compute hadronic transition matrix elements for arbitrary currents at leading order in $1/N_c$. We compute the semileptonic differential decay rate of a heavy meson, $d\Gamma/dx$, and its moments, M_N , using the hadronic matrix elements obtained previously. We put some emphasis in trying to understand parity invariance. We also study with special care the kinematic region where the operator product expansion ($1/N \sim 1 - x \sim 1$) or non-local effective field theories ($1/N \sim 1 - x \sim \Lambda_{QCD}/m_Q$) can be applied. We then compare with the results obtained using an effective field theory approach based on perturbative factorization, with the focus to better understand quark-hadron duality. At the end of the day, using effective field theories, we have been able to obtain expressions for the moments with relative accuracy of $O(\Lambda_{QCD}^2/m_Q^2)$ in the kinematic region where the operator product expansion can be applied, and with relative accuracy of $O(\Lambda_{QCD}/m_Q)$ in the kinematic region where non-local effective field theories can be applied. These expressions agree, within this precision, with those obtained from the hadronic result using the layer-function approximation plus Euler-McLaurin expansion. Very good numerical agreement for the moments is obtained between the exact result and the result using effective field theories.

PACS numbers: 12.38.Aw, 12.39.Hg, 13.20.He, 13.20.-v

*Permanent address after September 1st: Grup de Física Teòrica and IFAE, Universitat Autònoma de Barcelona, E-08193 Bellaterra, Barcelona, Spain.

Contents

1	Introduction	3
2	QCD₁₊₁ in the light front	5
2.1	The 't Hooft equation	7
2.2	Transition matrix elements	8
2.3	The static limit	11
3	Semileptonic differential decay rate	12
3.1	Kinematics	12
3.2	Differential decay rate: hadronic computation	16
3.3	Moments	24
4	SCETI: Multimode approach	30
4.1	Lagrangian and heavy-to-light current	33
4.2	Semileptonic differential decay rate	36
5	Soft-(Collinear) Effective Theory in $D = 1 + 1$	39
5.1	Semileptonic differential decay rate	43
6	Conclusions	48
A	Conventions and notation	50

1 Introduction

Asymptotic freedom can be seen as the first example of factorization between high and low energies, since it dictates that Green functions at high Euclidean energies (Q^2) can be described by perturbation theory up to corrections suppressed by powers of Λ_{QCD} over Q . Therefore, the use of the operator product expansion (OPE) in processes where the relevant momentum scale is large and Euclidean is safe. This is quite restrictive, since, in most of the cases, it can only be tested with experiment through dispersion relations, which involve measurements up to arbitrarily high energies. To avoid this problem what one usually does is to directly apply the same perturbative factorization techniques to observables living in the Minkowski regime. In practice this means to perform the analytic continuation of approximate perturbative results obtained in the Euclidean region to the Minkowski region. Nevertheless, such calculations do not come from first principles. This affects the OPE and effective field theories that are built using perturbative factorization techniques aiming to factorize high from low energies. This problem is usually stated as duality violations. We will follow here the definition of [1] for duality violations.

One can quantify the discrepancy between the exact result and the one using perturbative factorization in the large N_c limit of QCD [2]. In this case one finds a clear discrepancy between both results in the physical cut of the Green functions, where one has infinitely narrow resonances on the one hand and an smooth function on the other. This can be further quantified in the 't Hooft model [3], which we will consider in what follows¹. For this model, when one considers some inclusive quantities like the total heavy meson or tau decay rate, the discrepancies between the hadronic and OPE-like result (using the OPE for the tau decay and HQET for the inclusive heavy meson decay [4,5]) appear to be quite suppressed.

On the other hand one may also study more exclusive quantities like the differential cross section of the electron-meson scattering going to electron+anything: $eM \rightarrow eX$ (deep inelastic scattering), the differential semi-leptonic inclusive decays of heavy mesons: $H_Q \rightarrow Xl\nu$, or $e^+e^- \rightarrow$ light hadrons. Indeed one would expect that the magnitude of the duality violations for these quantities would be larger, since they are more exclusive observables. Some of them have been already studied in the literature [6,7], like deep inelastic scattering or $e^+e^- \rightarrow$ light hadrons. One finds that the violation of duality is maximal but that, if one makes some sort of smearing of the hadronic result, the partonic results are recovered at leading order. Nevertheless, for these observables, the partonic computation is performed at a diagrammatic level, which makes difficult to go beyond the leading order partonic result. In part this is so because one has to deal with jets (very energetic final states with relatively small invariant mass) in the final state. Moreover it is also difficult to quantify the error made by the smearing procedure, since the smeared function does not actually correspond to the differential cross section or decay anymore.

¹One may believe that the large N_c limit sets a kind of upper bound on the duality violations. In the real case, the existence of finite decay widths is expected to smooth the duality violations. However, at present, it is not possible to quantify this effect. In any case, this does not mean that one can use the results of the two-dimensional model as upper bounds to the four-dimensional case with finite N_c .

At this respect, there have been recent developments in order to apply effective field theories with perturbative factorization to jet physics in four dimensions. This is a rapidly evolving field [8,9,10,11,12] and the effective field theory has been called soft-collinear effective theory (SCET). The use of effective field theories with perturbative factorization may allow for a comparison between partonic and hadronic results in a more systematic way, beyond the leading order partonic result, and to set up a right framework on which to quantify the quark-hadron duality violations. Nevertheless, several questions still remain open in SCET, like what the modes of the theory are, or what the optimal formulation of this theory could be. The standard formulations of SCET involve the existence of a large number of modes, and one can never be sure that the set is complete. For instance, in Ref. [12] it has been argued that there could be some extra modes called *messenger*. There is no consensus on this issue, though, and in Refs. [13,14] it is claimed that there is no need for such modes. Therefore, it is evident that the study of SCET is interesting on its own and the application of SCET in a controlled setup may help to better understand the structure of the effective theory. Obviously, QCD_{1+1} provides this controlled setup. This will be one of the main subjects of this paper. On the side of the optimal formulation of SCET, we would like to incorporate the advantages of the light-front quantization frame [15] and the associated Hamiltonian-like formulation. This provides non-trivial information, since it allows to relate the correlators that appear in the effective theory with the wave-function of the bound state. It also avoids to perform complicated diagrammatic computations and resummation via Dyson-Schwinger equations to obtain the matrix elements and vertices (as it was done in Refs. [6,7]). Moreover, working in the light-cone gauge is convenient to make the theory effectively abelian in 1+1 dimensions.

The specific observable we will consider in this paper to illustrate the discussion will be the differential semileptonic inclusive decays of heavy mesons: $H_Q \rightarrow X l \nu$. We will only consider the kinematical situation when the invariant mass square of the jet, P_X^2 , is much larger than $\Lambda_{\text{QCD}}^2 \sim \beta^2$ (β^2 is the strong coupling, which has square mass dimensions in $D = 1+1$). In this situation we will see that one of the modes of SCET, the hard-collinear, is not a dynamical field and can be integrated out, at least in the light-front frame. The final effective theory becomes equal to HQET plus an imaginary vertex. This imaginary vertex is local in "time" (in the light-front quantization frame), can be computed order by order in perturbation theory, and is able to describe the differential decay rate (more precisely, the moments).

We structure the paper as follows. In sec. 2 we analyze QCD_{1+1} in the light front and compute the transition matrix elements. In sec. 3 we compute the hadronic differential decay rate and moments. In sec. 4, we work out SCET in two dimensions and compute the differential decay rate and moments at tree level. In sec. 5, we develop an alternative effective theory without hard-collinear fields and compute the differential decay rate and moments at one loop. In the Appendix we set up the notation and conventions.

2 QCD₁₊₁ in the light front

In $D = 1 + 1$, the QCD Lagrangian is given by

$$\mathcal{L}_{1+1} = -\frac{1}{4}G_{\mu\nu}^a G^{a,\mu\nu} + \sum_i \bar{\psi}_i (i\gamma^\mu D_\mu - m_i + i\epsilon) \psi_i, \quad (1)$$

where $D_\mu = \partial_\mu + igA_\mu$ and i labels the flavor.

One can perform the quantization in a frame different from the equal-time frame. In particular it is possible to choose the quantization frame at $x^+ = \text{constant}$, which would play the role of time in this case. The role of the energy is played by the conjugated variable P^- . The other variables: P^+ (and P_\perp in four dimensions) are kinematical. For instance, the P_H^+ component of an hadron behaves in "free"-particle way,

$$P_H^+ = \sum_i P_i^+, \quad (2)$$

where the sum extends over all the partonic components of the bound state. This allows to define the variable "x", which measures the fraction of P_H^+ momentum carried by a given parton.

The notation for the components of the gluon field is

$$A^+ \equiv n_+ \cdot A, \quad A^- \equiv n_- \cdot A. \quad (3)$$

The usual quantization gauge is $A^+(x) = 0$. In this situation, the fields $\psi_- = \Lambda_- \psi$ (for the definition of $\Lambda_{+/-}$ see the appendix) and A^- are non-dynamical and can be integrated out from the theory (they are constraints)². The resulting Lagrangian reads ($\psi_+ = \Lambda_+ \psi$)

$$\begin{aligned} \mathcal{L} = & \sum_i \psi_{i+}^\dagger i\partial^- \psi_{i+} + i \sum_i \frac{m_i^2 - i\epsilon}{4} \int dy^- \psi_{i+}^\dagger(x^-, x^+) \epsilon(x^- - y^-) \psi_{i+}(y^-, x^+) \\ & + \sum_{ij} \frac{g^2}{4} \int dy^- \psi_{i+}^\dagger t^a \psi_{i+}(x^-, x^+) |x^- - y^-| \psi_{j+}^\dagger t^a \psi_{j+}(y^-, x^+), \end{aligned} \quad (4)$$

where we have defined

$$\epsilon(x) = \begin{cases} -1, & x < 0, \\ 0, & x = 0, \\ 1, & x > 0. \end{cases} \quad (5)$$

The representation of the quarks in terms of free fields in the light-cone quantization frame reads

$$\psi_+(x) = \int_0^\infty \frac{dp^+}{2(2\pi)} (a(p)e^{-ipx} + b^\dagger(p)e^{ipx}), \quad (6)$$

²One should not forget that there is another constraint, the Gauss law, that restricts the Hilbert space of physical states to those which are singlet under gauge transformations. See for instance [16], where one can also find a quantization in the path integral formulation.

and the anticommuting relations are

$$\begin{aligned} \{a(p), a^\dagger(q)\} &= \{b(p), b^\dagger(q)\} = 2(2\pi)\delta(p^+ - q^+), \\ \{a(p), b^\dagger(q)\} &= \{b(p), a^\dagger(q)\} = 0. \end{aligned} \quad (7)$$

Once we have the Lagrangian we can construct the Hamiltonian (in the light-cone frame)

$$\begin{aligned} P^- &= -i \sum_i \frac{m_i^2 - i\epsilon}{4} \int dx^- dy^- \psi_{i+}^\dagger(x^-, x^+) \epsilon(x^- - y^-) \psi_{i+}(y^-, x^+) \\ &\quad - \sum_{ij} \frac{g^2}{4} \int dx^- dy^- \psi_{i+}^\dagger t^a \psi_{i+}(x^-, x^+) |x^- - y^-| \psi_{j+}^\dagger t^a \psi_{j+}(y^-, x^+). \end{aligned} \quad (8)$$

By solving the eigenstate equation (taking into account the constraints and where n schematically labels the quantum numbers of the bound state)

$$P^- |n\rangle = P_n^- |n\rangle, \quad (9)$$

one obtains the basis of states on which the Hilbert space of physical states can be spanned. Here we will focus on the meson sector of the Hilbert space and we will generically label the state as $|ij; n\rangle$, where i labels the flavor of the valence quark, j labels the flavor of the valence antiquark and n labels the excitation of the bound state. The solution to Eq. (9) can be obtained from the large N_c limit solutions within a systematic expansion in $1/N_c$ using standard time-independent quantum perturbation theory. It has the following structure (the momentum of the bound state will not be displayed explicitly unless necessary)

$$\begin{aligned} |ij; n\rangle &= |ij; n\rangle^{(0)} \\ &+ \sum_{m, n'} \sum_k |ik; n'\rangle^{(0)} |kj; m\rangle^{(0)(0)} \langle ik; n'|^{(0)} \langle kj; m| P^- |ij; n\rangle^{(0)} \frac{1}{P_n^{(0)-} - P_m^{(0)-} - P_{n'}^{(0)-}} \\ &+ O\left(\frac{1}{N_c}\right), \end{aligned} \quad (10)$$

where the second term in the expression is $1/\sqrt{N_c}$ suppressed. Here we have used the fact that, at order $1/\sqrt{N_c}$, P^- only connects neighboring sectors (n -mesons $\rightarrow n \pm 1$ -mesons), becoming an almost diagonal infinite dimensional matrix. $|ij; n\rangle^{(0)}$ represents the eigenstate solution to Eq. (9) in the large N_c limit, and $P_n^{(0)}$ the associated eigenvalue (we do not explicitly display the flavor content of $P_n^{(0)}$ except in cases where it can produce confusion). In this limit the sectors with fixed number of quarks and antiquarks are conserved and consequently the number of mesons. Therefore, the bound state can be represented in the following way

$$|ij; n\rangle^{(0)} = \frac{1}{\sqrt{N_c}} \int_0^{P_n^+} \frac{dp^+}{\sqrt{2(2\pi)}} \phi_n^{ij} \left(\frac{p^+}{P_n^+} \right) a_{i,\alpha}^\dagger(p) b_{j,\alpha}^\dagger(P_n - p) |0\rangle, \quad (11)$$

where α is the color index, ϕ_n^{ij} is the solution to the 't Hooft equation, which will be reviewed in the next section, and the state is normalized as

$${}^{(0)}\langle ij; m | i' j'; n \rangle^{(0)} = 2\pi 2P_n^{(0)+} \delta_{mn} \delta_{ii'} \delta_{jj'} \delta(P_m^{(0)+} - P_n^{(0)+}). \quad (12)$$

The fact that the number of particles is quasi-conserved makes possible to formulate the theory along similar lines of how is done in pNRQCD (for a review see [17]), where the wave function (the 't Hooft wave function in our case) is promoted to the status of being the field representing the bound state. We will not pursue this line of research further in this paper but we expect to come back to this issue in the future.

2.1 The 't Hooft equation

By applying the operator P^- to its eigenstate $|n\rangle$ at leading order in $1/N_c$ one obtains the 't Hooft equation

$$M_n^2 \phi_n^{ij}(x) = \hat{P}^2 \phi_n^{ij}(x) \equiv \left(\frac{m_{i,R}^2}{x} + \frac{m_{j,R}^2}{1-x} \right) \phi_n^{ij}(x) - \beta^2 \int_0^1 dy \phi_n^{ij}(y) P \frac{1}{(y-x)^2}, \quad (13)$$

where M_n is the bound state mass, $\beta^2 \equiv \frac{g^2 N_c}{2\pi}$, $x = p^+ / P_n^+$, with p^+ being the momentum of the quark i , and P stands for Cauchy's Principal Part³. The renormalized mass is given by $m_{i,R}^2 = m_i^2 - \beta^2$. The principal value prescription serves to regulate the integrand singularity, which originates in the infrared divergence of the gluon propagator. This equation has a discrete spectrum of eigenvalues that increase approximately linearly for large n , and the wave functions vanish at the boundaries with the asymptotic behavior

$$\phi_n^{ij}(x) \rightarrow x^{\beta_i}, \quad x \rightarrow 0, \quad (15)$$

where

$$m_{i,R}^2 + \pi \beta_i \cot \pi \beta_i = 0, \quad (16)$$

and similarly for $x \rightarrow 1$. The 't Hooft wavefunction are chosen to be normalized to unity

$$\int_0^1 dx \phi_n^{ij*}(x) \phi_n^{ij}(x) = \delta_{nm}. \quad (17)$$

We will have to consider high excitations of mesons when considering the decay rate of the heavy meson. In the asymptotic limit $n \rightarrow \infty$ one can obtain analytic expressions both for the masses

$$M_n^2 \simeq n\pi^2 \beta^2, \quad (18)$$

³One can use the following representation of this distribution

$$P \frac{1}{(x-y)^2} = -\frac{1}{2} \int_{-\infty}^{\infty} dz |z| e^{i(x-y)z}. \quad (14)$$

and for the meson wave functions

$$\phi_n^{ij}(x) \simeq \sqrt{2} \sin(n\pi x) . \quad (19)$$

Actually, a more detailed study of the 't Hooft equation has been performed in the large n limit using semiclassical (WKB approximation) techniques in Ref. [18]. In this reference the layer function was defined (see also [7]):

$$\phi_i(\xi) \equiv \lim_{n \rightarrow \infty} \phi_n^{ij}(\xi/M_n^2) , \quad (20)$$

for finite ξ . This function is the solution of the equation

$$\phi_i(\xi) = \frac{m_{i,R}^2}{\xi} \phi_i(\xi) - \beta^2 \int_0^\infty d\xi' \phi_i(\xi') \mathbb{P} \frac{1}{(\xi' - \xi)^2} , \quad (21)$$

and the following equalities can be obtained

$$\int_0^\infty d\xi \frac{\phi_i(\xi)}{\xi} = \pi \frac{\beta}{m_i} , \quad \int_0^\infty d\xi \phi_i(\xi) = \beta \pi m_i , \quad (22)$$

which we will need in the following sections.

2.2 Transition matrix elements

We are now in the position to compute the transition matrix elements due to an arbitrary current:

$$\langle cs; m | \bar{\psi}_c \Gamma Q | Qs; n \rangle , \quad (23)$$

where Γ represents a generic Dirac matrix. We anticipate the notation that we will use for the heavy meson decay: Q represents the field of the heavy quark as well as its flavor, s the flavor of the spectator quark and c the flavor of the hard-collinear quark. We will restrict ourselves to the kinematical situation relevant for the semileptonic heavy meson decay. This means that $P_m^+ \leq P_n^+$ and $P_m^- \leq P_n^-$.

We only aim to obtain the matrix element (23) at leading order in $1/N_c$. Nevertheless, this does not mean that we can just work with the leading order solution to the bound states. As we will see, we will also need the $1/\sqrt{N_c}$ corrections to the bound state. The contribution to the matrix element (23) can be split into two contributions. We distinguish the contributions to the current according to whether they come from "diagonal" or "off-diagonal" terms, which we show in Fig. 1. The diagonal term directly connects the current to the leading $O(1/N_c^0)$ term of the bound state:

$$\langle cs; m | \bar{\psi}_c \Gamma Q | Qs; n \rangle |_{diag.} = {}^{(0)} \langle cs; m | \bar{\psi}_c \Gamma Q | Qs; n \rangle^{(0)} . \quad (24)$$

This term is of $O(1/N_c^0)$ and it is produced from terms of the type $\bar{\psi}_c \Gamma Q \sim b_c a_Q^\dagger + \dots$. In a way they change the flavor of the bound state from "heavy" to "hard-collinear". Nevertheless, there is another possibility: $\bar{\psi}_c \Gamma Q \sim b_c b_Q + \dots$, which can be understood as

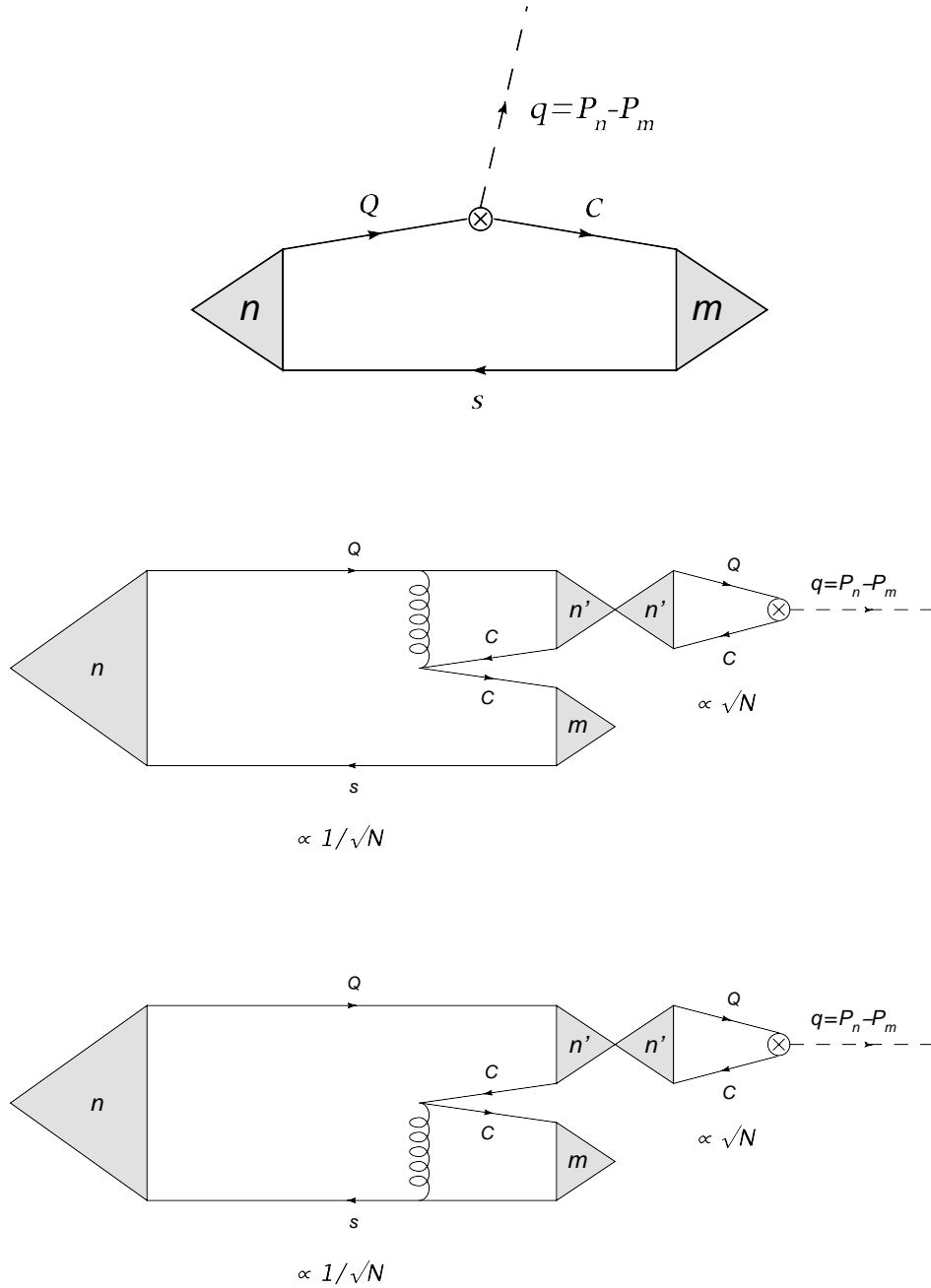


Figure 1: Contributions to the hadronic matrix elements of the current. The first figure corresponds to the "diagonal" contribution to the matrix element, Eq. (24). The second and third figures correspond to the "off-diagonal" terms, Eq. (25). The \otimes represents the current, and the gluon exchange the effective four-fermion interaction in Eq. (8).

the creation (annihilation) of a new bound state. This possibility does not have overlap with the leading order term in the $1/N_c$ expansion of the bound state but it does with the $1/\sqrt{N_c}$ one. Whereas the matrix element connecting the one meson sector with the two meson sector is $1/\sqrt{N_c}$ suppressed, the overlap of the two meson state with the current is $\sqrt{N_c}$ enhanced. This is why this contribution has to be considered as well at leading order in $1/N_c$. We define

$$\begin{aligned} \langle cs; m | \bar{\psi}_c \Gamma Q | Qs; n \rangle |_{off-diag.} &= \sum_{n'} \int \frac{dP_{n'}^+}{2(2\pi)P_{n'}^+} \frac{1}{P_n^{(0)-} - P_m^{(0)-} - P_{n'}^{(0)-}} \quad (25) \\ &\times \langle 0 | \bar{\psi}_c \Gamma Q | Qc; n' \rangle^{(0)(0)} \langle Qc; n' |^{(0)} \langle cs; m | P^- | Qs; n \rangle^{(0)}. \end{aligned}$$

A good thing of working this way is that, once $\langle 0 | \bar{\psi}_c \Gamma Q | Qc; n' \rangle^{(0)(0)} \langle cs; m | P^- | Qs; n \rangle^{(0)}$ has been computed, it can be used for any current. The total result for the matrix element at leading order in $1/N_c$ then reads

$$\langle cs; m | \bar{\psi}_c \Gamma Q | Qs; n \rangle = \langle cs; m | \bar{\psi}_c \Gamma Q | Qs; n \rangle |_{diag.} + \langle cs; m | \bar{\psi}_c \Gamma Q | Qs; n \rangle |_{off-diag.}. \quad (26)$$

We are now in the position to apply the above discussion to some specific currents. We display the results below ($x = q^+ / P_n^+ = (P_n^+ - P_m^+) / P_n^+$).

$$\begin{aligned} \langle cs; m | \bar{\psi}_c \gamma^+ Q | Qs; n \rangle &= 2 \langle cs; m | \psi_{+,c}^\dagger Q_+ | Qs; n \rangle \quad (27) \\ &= 2P_n^+(1-x) \left[\int_0^1 dz \phi_n^{Qs}(x+(1-x)z) \phi_m^{cs}(z) \right. \\ &\quad \left. - x^2 \beta^2 \int_0^1 \int_0^1 dudz \frac{\phi_m^{cs}(z) G(u; q^2)}{(x(1-u) + (1-x)z)^2} (\phi_n^{Qs}(x+(1-x)z) - \phi_n^{Qs}(xu)) \right], \end{aligned}$$

$$G(u; q^2) \equiv \int_0^1 dv \sum_{n'=0}^{\infty} \frac{\phi_{n'}^{Qc}(u) \phi_{n'}^{Qc}(v)}{q^2 - M_{n'}^2}. \quad (28)$$

$$\begin{aligned} \langle cs; m | \bar{\psi}_c \gamma^- Q | Qs; n \rangle &= 2 \langle cs; m | \left(\frac{m_c}{i\partial^+} \psi_{c,+} \right)^\dagger \left(\frac{m_Q}{i\partial^+} Q_+ \right) | Qs; n \rangle \quad (29) \\ &= \frac{2m_Q m_c}{P_n^+} \int_0^1 dz \frac{\phi_n^{Qs}(x+(1-x)z) \phi_m^{cs}(z)}{(x+(1-x)z)z} + 2\beta^2 \frac{1-x}{P_n^+} \sum_{n'=0}^{\infty} \frac{(-1)^{n'} M_{n'}^2}{q^2 - M_{n'}^2} \\ &\quad \times \int_0^1 \int_0^1 \int_0^1 dy dt dz \frac{\phi_{n'}^{Qc}(y) \phi_m^{cs}(t) \phi_{n'}^{Qc}(z)}{(t(1-x) + (1-z)x)^2} (\phi_n^{Qs}(x+(1-x)t) - \phi_n^{Qs}(xz)). \end{aligned}$$

$$\begin{aligned} \langle cs; m | \bar{\psi}_c Q | Qs; n \rangle &= \int_0^1 dz \phi_n^{Qs}(x+(1-x)z) \phi_m^{cs}(z) \left(\frac{m_Q(1-x)}{x+(1-x)z} + \frac{m_c}{z} \right) \\ &\quad - \beta^2 \frac{x(1-x)}{m_Q - m_c} \sum_{n' \text{ odd}} \frac{M_{n'}^2}{q^2 - M_{n'}^2} \quad (30) \\ &\quad \times \int_0^1 \int_0^1 \int_0^1 dy dt dz \frac{\phi_{n'}^{Qc}(y) \phi_m^{cs}(t) \phi_{n'}^{Qc}(z)}{(t(1-x) + (1-z)x)^2} (\phi_n^{Qs}(x+(1-x)t) - \phi_n^{Qs}(xz)). \end{aligned}$$

The "+" component of the vector current was already computed in Ref. [7]. The computation of the rest of the matrix elements had to wait to Ref. [19], but we disagree with their results for the "-" component of the vector current and for the scalar current. More recently, expressions for the transition matrix elements of the current have also been worked out in Ref. [20]. We find that our expressions are more compact than those. In any case we have not been able to check the agreement with those. In Ref. [21] the matrix elements have also been considered using similar techniques to ours. Nevertheless, they consider different kinematics, which makes difficult the comparison with their results.

Finally, we would like to stress that current conservation imposes strong constraints on the form of the currents. The following equalities have to be fulfilled between the different matrix elements

$$q_\mu \langle cs; m | \bar{\psi}_c \gamma^\mu Q | Qs; n \rangle = (m_Q - m_c) \langle cs; m | \bar{\psi}_c Q | Qs; n \rangle, \quad (31)$$

where $q^\mu = P_n^\mu - P_m^\mu$. For the case in which the hard-collinear and the heavy quark correspond to the same particle, and taking the limit $q^2, x \rightarrow 0$, we obtain the equality (first obtained in Ref. [22])

$$\int_0^1 \frac{(\phi_n^{ij})^2(x)}{x^2} = \frac{M_n^2}{m_{i,R}^2} \int_0^1 (\phi_n^{ij})^2(x) = \frac{M_n^2}{m_{i,R}^2}. \quad (32)$$

2.3 The static limit

Since in this paper we will study the differential decay rate of a heavy meson, it is convenient to consider the specific case on which one of the quarks is very heavy (the static limit). If we redefine the heavy quark field,

$$Q_+ = e^{-im_Q v \cdot x} Q_{+v}, \quad (33)$$

where in the infinite mass limit one can use ($p = m_Q v + k$)

$$Q_{+v}(x) = \int \frac{dk^+}{2(2\pi)} a_v(k) e^{-ikx}, \quad (34)$$

at leading order in $1/m_Q$ the Lagrangian reads

$$\begin{aligned} \mathcal{L}_{static} = & \sum_i \psi_{i+}^\dagger i \partial^- \psi_{i+} + i \sum_i \frac{m_i^2 - i\epsilon}{4} \int dy^- \psi_{i+}^\dagger(x^-, x^+) \epsilon(x^- - y^-) \psi_{i+}(y^-, x^+) \\ & + Q_{+v}^\dagger (i \partial^- + i \partial^+ + i\epsilon) Q_{+v} \\ & + \frac{g^2}{4} \sum_{ij} \int dy^- \psi_{i+}^\dagger t^a \psi_{i+}(x^-, x^+) |x^- - y^-| \psi_{j+}^\dagger t^a \psi_{j+}(y^-, x^+) \\ & + \frac{g^2}{2} \sum_i \int dy^- \psi_{i+}^\dagger t^a \psi_{i+}(x^-, x^+) |x^- - y^-| Q_{+v}^\dagger t^a Q_{+v}(y^-, x^+). \end{aligned} \quad (35)$$

In the same way we can obtain the Hamiltonian in the static limit (at leading order in the $1/m_Q$ expansion)

$$\begin{aligned}
P_{static}^- &= -i \sum_i \frac{m_i^2}{4} \int dx^- dy^- \psi_{i+}^\dagger(x^-, x^+) \epsilon(x^- - y^-) \psi_{i+}(y^-, x^+) - Q_{+v}^\dagger (-i\partial^-) Q_{+v} \\
&\quad - \frac{g^2}{4} \sum_{ij} \int dy^- \psi_{i+}^\dagger t^a \psi_{i+}(x^-, x^+) |x^- - y^-| \psi_{j+}^\dagger t^a \psi_{j+}(y^-, x^+) \\
&\quad - \frac{g^2}{2} \sum_i \int dy^- \psi_{i+}^\dagger t^a \psi_{i+}(x^-, x^+) |x^- - y^-| Q_{+v}^\dagger t^a Q_{+v}(y^-, x^+). \tag{36}
\end{aligned}$$

Once this Hamiltonian is applied to mesonic states, one obtains the 't Hooft equation in the static limit for which one can find a thorough study in Ref. [23]. In this limit, one works with the function $\Psi_n^i(t) = \frac{1}{\sqrt{m_Q}} \phi_n^{Q_i} \left(1 - \frac{t}{m_Q}\right)$, where $t = (1-x)m_Q$, and considers its static limit, which is described by the following equation ($\epsilon_n = M_n - m_Q$, neglecting $1/m_Q$ corrections):

$$\epsilon_n \Psi_n^i(t) = \frac{m_i^2 - \beta^2}{2t} \Psi_n^i(t) + \frac{t}{2} \Psi_n^i(t) - \frac{\beta^2}{2} \int_0^\infty ds \frac{\Psi_n^i(s)}{(t-s)^2}. \tag{37}$$

The quantities that will be needed in the following are expectation values of the variable t in the static limit, defined in terms of the heavy meson wave function,

$$\langle t^r \rangle \equiv \int_0^\infty dt (\Psi_n^s(t))^2 t^r. \tag{38}$$

The numerical computation of these expectation values can be cross-checked with the help of static limit sum rules [23] such as

$$\langle t \rangle = \epsilon_n, \tag{39}$$

$$\langle t^2 \rangle = \frac{4}{3} \langle t \rangle^2 - \frac{1}{3} (m_s^2 - \beta^2). \tag{40}$$

The above expressions will be useful in the computation of the OPE expansions of the differential decay rate moments, see sec. 3.3.

3 Semileptonic differential decay rate

3.1 Kinematics

We consider here the semileptonic heavy meson decay: $H_Q \rightarrow X_c l_a \bar{l}_b$, where H_Q represents a bound state made of a heavy quark Q and a light (spectator) quark s (by default we will perform the numerical analysis for the ground state but the formulas hold for any

state). X_c represents any hadronic final state with c (hard-collinear) flavour content and $l_{a,b}$ represent massless leptons. We will consider the situation on which the spectator, ψ_s , and hard-collinear, ψ_c , quarks have different flavour in order to avoid annihilation and Pauli interference terms. This decay has already been studied in the past. We will follow here the work of Bigi et al. [4]. The authors considered the flavour changing weak interaction

$$\mathcal{L}_{\text{weak}}^V = -\frac{G}{\sqrt{2}}\bar{\psi}_c\gamma_\mu Q\bar{l}_a\gamma^\mu l_b. \quad (41)$$

The total decay width can be written as

$$\Gamma_{H_Q} = \frac{G^2}{M_{H_Q}} \int \frac{d^2q}{(2\pi)^2} \theta(q^+) \theta(q^-) \text{Im} \Pi_{\mu\nu}(q) \text{Im} T^{\mu\nu}(q), \quad (42)$$

where $\Pi_{\mu\nu}(x)$ and $T_{\mu\nu}(x)$ are defined as

$$\Pi_{\mu\nu}(x) = i \langle 0 | T \{ \bar{l}_a(x) \gamma_\mu l_b(x) \bar{l}_b(0) \gamma_\nu l_a(0) \} | 0 \rangle, \quad (43)$$

$$T^{\mu\nu}(x) = i \langle H_Q | T \{ \bar{Q}(x) \gamma^\mu \psi_c(x) \bar{\psi}_c(0) \gamma^\nu Q(0) \} | H_Q \rangle, \quad (44)$$

and their Fourier transform as

$$\Pi_{\mu\nu}(q) = \int d^2x e^{iqx} \Pi_{\mu\nu}(x), \quad T^{\mu\nu}(q) = \int d^2x e^{-iqx} T^{\mu\nu}(x). \quad (45)$$

The imaginary part of $\Pi_{\mu\nu}(q)$ reads

$$\text{Im} \Pi^{\mu\nu}(q) = q^\mu q^\nu \delta(q^2) = \begin{cases} q^+ \delta(q^-) & (+, +) \text{ component,} \\ q^- \delta(q^+) & (-, -) \text{ component,} \\ 0 & \text{otherwise.} \end{cases} \quad (46)$$

We notice that the result Eq. (46) is the same in the equal-time or in the light-front formalism. This is so in the massless case. Once masses are included the situation becomes more complicated. One may wonder how it is possible to obtain the term proportional to $\delta(q^+)$ and *finite* $q^- = P_a^- + P_b^- = m_a^2/P_a^+ + m_b^2/P_b^+$ in the leptonic correlator for massless leptons. This is somewhat amusing if one works in the light-front quantization frame. Naively one would expect that q^- is always zero if the masses of the leptons are zero. Nevertheless, one may obtain $\text{Im} \Pi^{--} = q^- \delta(q^+)$ (which is necessary to restore parity invariance) by working with finite masses for the leptons and taking the massless limit at the very end. Being more precise, this contribution appears from very high $P_{a,b}^+$, scaling like $P_{a,b}^+ \sim \tilde{P}_{a,b}^+/m_{a,b}^2$ with $\tilde{P}_{a,b}^+$ finite.

We can see that two terms are generated for the differential decay rate (where M_{H_Q} is the mass of the H_Q meson):

$$\frac{d\Gamma^{(+)}}{dx} \equiv \frac{G^2 M_{H_Q}}{2(4\pi)^2} x \text{Im} T^{--}(q^- = 0, q^+) \quad (47)$$

with $x = q^+/M_{H_Q} \geq 0$, and

$$\frac{d\Gamma^{(-)}}{dx} \equiv \frac{G^2 M_{H_Q}}{2(4\pi)^2} x \text{Im} T^{++}(q^-, q^+ = 0) \quad (48)$$

with $x = q^-/M_{H_Q} \geq 0$. The total decay width then reads

$$\Gamma_{H_Q} = \int_0^1 dx \left(\frac{d\Gamma^{(+)}}{dx} + \frac{d\Gamma^{(-)}}{dx} \right). \quad (49)$$

The procedure of Ref. [4] was to assume that

$$\frac{d\Gamma^{(+)}}{dx} = \frac{d\Gamma^{(-)}}{dx} \equiv \frac{1}{2} \frac{d\Gamma}{dx} \quad (50)$$

are equal by parity symmetry and only to compute $\frac{d\Gamma^{(-)}}{dx}$. That both terms are equal is indeed highly non-trivial due to the fact that the gauge fixing $A^+ = 0$ and working in the light-front quantization frame breaks the explicit invariance under parity. We will here explicitly compute $\frac{d\Gamma^{(+)}}{dx}$ and compare with $\frac{d\Gamma^{(-)}}{dx}$. We then have to compute the differential decay rate (in Ref. [4] only the total decay rate was considered). As we will see, its computation is highly non trivial and requires to take the massless limit for the hard-collinear quark in a careful way.

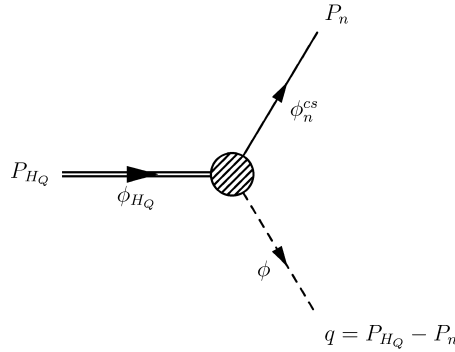


Figure 2: Decay of the heavy meson H_Q to the meson $|cs; n\rangle$ and the fictitious ϕ particle.

Eq. (46) shows that, at the practical level, the interaction could be simulated by a massless particle. Therefore, there are some kinematical similarities with a kind of $b \rightarrow X_c \gamma$ decay. The effective interaction would read [4]

$$\mathcal{L}_{\text{weak}}^V = -\frac{G}{\sqrt{2}\pi} \bar{\psi}_c \gamma_\mu Q \epsilon^{\mu\nu} (\partial_\nu \phi) + (h.c.), \quad (51)$$

where ϕ represents a fictitious pseudoscalar particle. The process can be seen in Fig. 2. Since the pseudoscalar particle is real, we can parametrize its two-momentum q as (for definiteness we set the kinematics relevant for the computation of $\frac{d\Gamma^{(+)}}{dx}$, for $\frac{d\Gamma^{(-)}}{dx}$ things work analogously)

$$q^0 = \frac{xM_{H_Q}}{2}, \quad q^1 = \frac{xM_{H_Q}}{2}, \quad q^- = 0, \quad (52)$$

where, by momentum conservation, the momentum of the final hadronic state $P_X = P_n$ reads

$$P_X^0 = \frac{M_{H_Q}}{2}(2-x), \quad P_X^1 = -q^1, \quad P_X^2 = M_{H_Q}^2(1-x). \quad (53)$$

In light-cone coordinates

$$P_X^- = P_X^0 - P_X^1 = M_{H_Q}, \quad P_X^+ = P_X^0 + P_X^1 = M_{H_Q}(1-x), \quad (54)$$

so we see that in the endpoint region $x \rightarrow 1$, the factor

$$\sqrt{1-x} = \sqrt{\frac{P_X^2}{M_{H_Q}^2}} \equiv \bar{\lambda} \quad (55)$$

is small. It will play the role of one of the SCET expansion parameter, and leads to appropriate scalings for the momentum of the final meson state:

$$P_X^- \sim 1, \quad P_X^+ \sim \bar{\lambda}^2, \quad (56)$$

which behaves as a collinear jet.

The heavy quark mass will be considered to be a large parameter (equivalent to Q in jet physics or deep inelastic scattering). We can distinguish at least three kinematical regimes (we use the names SCETI and SCETII for an easier comparison with the notation used in effective field theories, see next sections and Ref. [26]):

- a) OPE; $P_X^2 = M_n^2 = M_{H_Q}^2(1-x) \sim m_Q^2 \gg m_Q \Lambda_{\text{QCD}}$; $n \sim m_Q^2/g^2$,
- b) SCETI; $P_X^2 = M_n^2 = M_{H_Q}^2(1-x) \sim m_Q \Lambda_{\text{QCD}}$; $n \sim m_Q/g$,
- c) SCETII; $P_X^2 = M_n^2 = M_{H_Q}^2(1-x) \sim \Lambda_{\text{QCD}}^2$; $n \sim 1$.

One usually refers to situation c) as the most exclusive and a) as the less exclusive one. Here we would like to stress that in the large N_c limit (irrespectively of the number of spatial-time dimensions) all the three situations are equally exclusive, since they correspond to only one physical hadronic final state. n represents the principal quantum number of the hadronic excitation (we are having in mind a linear Regge behavior). Indeed, the jet multiplicity of the hadronic final state is not well represented in the large N_c .

We have two independent expansion parameters: $\lambda = \sqrt{\frac{\Lambda}{M_{H_Q}}}$ and $\bar{\lambda} = \sqrt{1-x}$. We note that $\lambda \ll 1$ is always fulfilled. With respect $\bar{\lambda}$, we will restrict ourselves to the situation where we are either in the OPE or SCETI situation.

Let us note at this stage that we are actually using the opposite kinematic condition to the one used in Ref. [4]. There is a reason for that. In our kinematics, the "energy" $P_{\bar{X}}$ of the hadronic jet is much larger than Λ_{QCD} . Therefore, in the "time"-axis, x^+ , the interaction takes place at very short times and can be considered local. This is what it will allow us to write the interaction as a local term (in "time", i.e. x^+) when we try to represent the process by means of effective field theories later on. See Fig. 13. This will also allow us to write the matrix elements in terms of the wave-function of the bound state. We will elaborate on this in secs. 4 and 5.

3.2 Differential decay rate: hadronic computation

We can use the spectral decomposition to relate $\text{Im}T$ with the transition matrix elements of the currents we computed in sec. 2.2. We obtain (we have already restricted to q^+ , $q^- \geq 0$)

$$\begin{aligned} \text{Im}T^{\mu\nu}(q) &= (2\pi)^2 \sum_n \int \frac{dP_n^+}{(2\pi)2P_n^+} \delta(-q^+ + P_{H_Q}^+ - P_n^+) \delta(-q^- + P_{H_Q}^- - P_n^-) \\ &\times \langle H_Q | \bar{Q}(0) \gamma^\nu \psi_c(0) | cs; n, P_n^+ \rangle \langle cs; n, P_n^+ | \bar{\psi}_c(0) \gamma^\mu Q(0) | H_Q \rangle. \end{aligned} \quad (57)$$

The expression for the differential decay rate then reads (we work in the rest frame of the heavy meson with $P_{H_Q}^+ = P_{H_Q}^- = M_{H_Q} = P_n^-$ and $x = 1 - P_n^+/P_{H_Q}^+ = 1 - M_n^2/M_{H_Q}^2$)

$$\frac{d\Gamma^{(+)}}{dx} = \frac{G^2 M_{H_Q}}{32\pi} \sum_{M_n \leq M_{H_Q}} \frac{x}{P_{H_Q}^+(1-x)} \left| \langle n; P_n^+ | \bar{\psi}_c(0) \gamma^- Q(0) | H_Q \rangle \right|^2 \delta(P_{H_Q}^- - P_n^-), \quad (58)$$

where the matrix element can be read from Eq. (29) taking the limit $q^2 \rightarrow 0$. We notice that the differential decay rate consists of a sum over deltas at the position of the resonances and, therefore, cannot be obtained from perturbative-like computations.

We could also do the computation with the kinematics $q^+ = 0$, $q^- = xM_{H_Q}$, along the lines of Ref. [4]. This is the "spatial" component of the momentum. In this case we would obtain ($P_{H_Q}^+ = P_{H_Q}^- = M_{H_Q} = P_n^+$ and $x = 1 - P_n^-/P_{H_Q}^- = 1 - M_n^2/M_{H_Q}^2$)

$$\frac{d\Gamma^{(-)}}{dx} = \frac{G^2}{32\pi} \sum_{M_n \leq M_{H_Q}} x \left| \langle n; P_n^+ | \bar{\psi}_c(0) \gamma^+ Q(0) | H_Q \rangle \right|^2 \delta(P_{H_Q}^- - P_n^- - q^-). \quad (59)$$

Note that in this case we have to compute the matrix elements in the limit $q^2, P_{H_Q}^+ - P_n^+ \rightarrow 0$, which considerably simplifies the computation and one obtains

$$\frac{d\Gamma^{(-)}}{dx} = \sum_{M_n \leq M_{H_Q}} \frac{\Gamma_n}{2} \delta\left(x - 1 + \frac{M_n^2}{M_{H_Q}^2}\right) \quad (60)$$

for the differential decay rate, where Γ_n is

$$\Gamma_n = \frac{G^2 M_{H_Q}^2 - M_n^2}{4\pi M_{H_Q}} \left[\int_0^1 dz \phi_n^{cs}(z) \phi_{H_Q}(z) \right]^2. \quad (61)$$

In principle, this expression should be equal to Eq. (58) for all x . This implies the following remarkable identity among matrix elements ($x_n = 1 - M_n^2/M_{H_Q}^2$)

$$\begin{aligned} \left| \int_0^1 dz \phi_n^{cs}(z) \phi_{H_Q}(z) \right| &= \left| \frac{m_Q m_c}{(P_{H_Q}^+)^2} \int_0^1 dz \frac{\phi_{H_Q}(x_n + (1-x_n)z) \phi_n^{cs}(z)}{(x_n + (1-x_n)z)z} \right. \\ &- \beta^2 \frac{1-x_n}{(P_{H_Q}^+)^2} \sum_{n'=0}^{\infty} (-1)^{n'} \int_0^1 \int_0^1 \int_0^1 dy dt dz \frac{\phi_{n'}^{Qc}(y) \phi_n^{cs}(t) \phi_{n'}^{Qc}(z)}{(t(1-x_n) + (1-z)x_n)^2} \\ &\left. \times (\phi_{H_Q}(x_n + (1-x_n)t) - \phi_{H_Q}(x_n z)) \right|. \end{aligned} \quad (62)$$

In the left-hand-side (LHS) of the equality only the "diagonal" term of the "+" current contributes. For the right-hand-side (RHS), the first term is the "diagonal" contribution of the "-" current and the second term is the "off-diagonal" one. Note that, in principle, we cannot fix the relative sign between both matrix elements. Note also that the equality Eq. (62) provides different information than Eq. (31), since it relates matrix elements with different "x" ($P_{H_Q}^+ - P_n^+ = 0$ in the LHS of the equation and $P_{H_Q}^+ - P_n^+ = x M_{H_Q}$ in the RHS of the equation). We have not been able to find a general analytic proof of these remarkable identities, though we have been able to do some partial checks, either when we have considered moments, or by using the layer functions for the final state (this implicitly assumes that we are working with a final state with a large quantum number n). In those cases we have been able to perform a comparison within an expansion in $1/m_Q$ and check the low order terms in this expansion. Irrespectively of the above, we have been able to check the equality (62) numerically to a level below the 1 % using the numerical solution to the 't Hooft equation obtained from the Brower-Spence-Weis improvement of the Mulhopp technique [18]. We have used two set of values for the masses of the quarks: $m_Q = 15\beta$, $m_c = 10\beta$, $m_s = 0.56\beta$ and $m_Q = 10\beta$, $m_c = \beta$, $m_s = \beta$. We show the comparison in Tables 1 and 2. This agreement is quite remarkable if we take into account that the support functions in both integrals are quite different (see Fig. 3), specially for the second set of parameters. Note that we do not consider the second term of the RHS of Eq. (62) in the plot. This term appears to be a correction compared with the first one and vanishes in the limit $m_Q \rightarrow \infty$. This is illustrated in Tables 1 and 2, where this second term appears to be smaller for larger values of the heavy quark mass. This points to the fact that their scaling may go like $\sim \beta^2/m_Q^2$ and that there are no terms of the type $\sim m_c^2/m_Q^2$. The convergence of this second term is very slow. One has to sum over a very large number of states to converge to the final value. We illustrate this problem in Fig. 4, where the sum is over 100 states.

n	LHS	RHS ("diag" term)	Rel. Err.	RHS	Rel. Err.
0	0.96433	0.97144	$7 \cdot 10^{-3}$	0.96627	$2 \cdot 10^{-3}$
1	0.25999	0.26175	$6 \cdot 10^{-3}$	0.26025	$1 \cdot 10^{-3}$
2	0.04432	0.04473	$9 \cdot 10^{-3}$	0.04445	$3 \cdot 10^{-3}$
3	0.02389	0.02405	$7 \cdot 10^{-3}$	0.02391	$1 \cdot 10^{-3}$
4	0.00543	0.00538	$7 \cdot 10^{-3}$	0.00540	$3 \cdot 10^{-3}$

Table 1: Values for the matrix elements as defined in Eq. (62). The first column corresponds to the principal quantum number. The second column corresponds to the left-hand side of the equality. The third column corresponds to the first term of right-hand side of the equality (the "diagonal" term). The fourth column to the relative difference between the second and third column. The fifth column corresponds to the right-hand side of Eq. (62) and the last column to the relative difference between the left and right-hand side of Eq. (62). In order to ease the comparison with the results of Lebed and Uraltsev [5], we take $m_Q = 15\beta$, $m_c = 10\beta$ and $m_s = 0.56\beta$.

n	LHS	RHS ("diag" term)	Rel. Err.	RHS	Rel. Err.
0	0.46946	0.42992	$9 \cdot 10^{-2}$	0.46493	$8 \cdot 10^{-3}$
1	0.61406	0.62957	$2 \cdot 10^{-2}$	0.61537	$2 \cdot 10^{-3}$
2	0.49594	0.51617	$4 \cdot 10^{-2}$	0.49821	$3 \cdot 10^{-3}$
3	0.32820	0.34773	$6 \cdot 10^{-2}$	0.32985	$5 \cdot 10^{-3}$
4	0.18571	0.19712	$6 \cdot 10^{-2}$	0.18694	$6 \cdot 10^{-3}$

Table 2: As in Table 1 with the values $m_Q = 10\beta$, $m_c = \beta$, $m_s = \beta$.

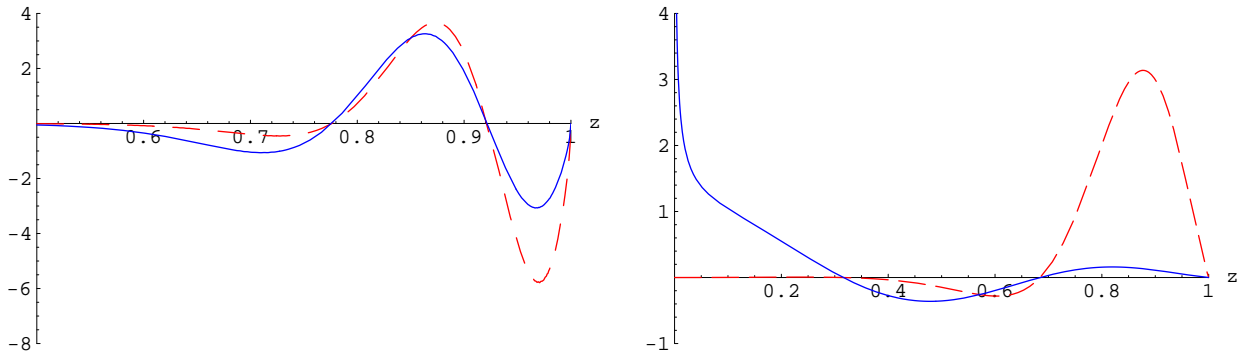


Figure 3: Plot of the integrands of Eq. (62). We have taken the values $n = 3$ and $m_c = 10\beta$, $m_s = 0.56\beta$ and $m_Q = 15\beta$ in the first figure and $m_c = 1\beta$, $m_s = 1\beta$ and $m_Q = 10\beta$ in the second figure. The dashed red line corresponds to the integrand of the left-hand side of the equality. The solid blue line corresponds to the integrand of the first term (the second term is subleading in $1/m_Q$ and it is not considered in this plot) of the right-hand side of the equality. In the first figure the solid blue line diverges (although in an integrable manner) for $z \rightarrow 0$ but it cannot be seen with the resolution of the plot.

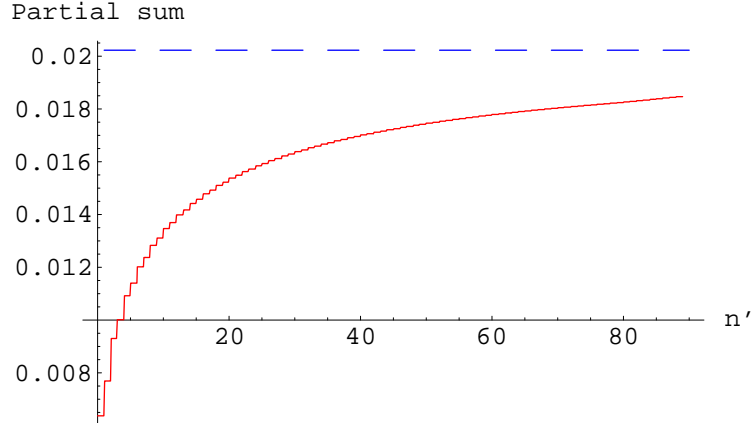


Figure 4: Analysis of the (off-diagonal) second term in the right-hand side of Eq. (62). We have taken the values $n = 3$ and $m_c = \beta$, $m_s = \beta$ and $m_Q = 10\beta$. The dashed blue line corresponds to the difference between the left and right hand side of the equality if the off-diagonal term is neglected. The solid red line represents the contribution of the off-diagonal term as a function of the number of intermediate states added to the sum. For n' larger than 80 the numerical stability of the computation is doubtful.

We are also able to compare with the numerical evaluation of the matrix elements (the LHS of Eq. (62)) performed in Ref. [5]. We have checked that our results agree with

theirs within the expected numerical uncertainties.

We would also like to remark that the RHS of Eq. (62) can be understood as a function of x , which for $x = x_n$ is equal to the LHS. Therefore, it provides with a definition of a continuous function in x . This will be relevant later on when trying to connect with computations using effective field theories.

So far these expressions are exact. At this stage we can perform an expansion in $1/m_Q$ and consider the large n limit (therefore our result will hold for the OPE or SCETI region but not for the SCETII kinematical situation). At lowest order in those expansions, and using the properties of the layer function defined in sec. 2.1, we obtain for the "diagonal" term of the matrix element (we also include the subleading corrections in m_c/m_Q , which can also be reliably computed with the layer function)

$$\begin{aligned}
& \frac{m_Q m_c}{M_{H_Q}^2} \int_0^1 dz \frac{\phi_{H_Q}(x + (1-x)z) \phi_n^{cs}(z)}{(x + (1-x)z)z} = \frac{m_Q}{M_{H_Q}^2} \int_x^1 dy \frac{\phi_{H_Q}(y)}{y} \frac{m_c}{y-x} \phi_n^{cs} \left(\frac{y-x}{1-x} \right) \\
& \simeq \frac{m_Q m_c}{M_{H_Q}^2} \left(\frac{\phi_{H_Q}(x)}{x} \int_0^\infty \frac{d\xi}{\xi} \phi_c(\xi) + \phi'_{H_Q}(x) \frac{1}{M_n^2} \frac{1-x}{x} \int_0^\infty d\xi \phi_c(\xi) \right. \\
& \quad \left. - \frac{\phi_{H_Q}(x)}{x^2} \frac{1-x}{M_n^2} \int_0^\infty d\xi \phi_c(\xi) \right) + \dots \\
& = \frac{m_Q}{M_{H_Q}^2} \frac{\phi_{H_Q}(x)}{x} \pi\beta \left(1 + \frac{m_c^2}{M_{H_Q}^2} \frac{\phi'_{H_Q}(x)}{\phi_{H_Q}(x)} - \frac{1}{x} \frac{m_c^2}{M_{H_Q}^2} + \dots \right)
\end{aligned} \tag{63}$$

by defining

$$\frac{y-x}{1-x} = \frac{\xi}{M_n^2} \tag{64}$$

and expanding in $1-x$.

We would like to stress that both the LHS and RHS of Eq. (63) can be defined for any x and not only for $x = x_n$. Nevertheless, they correspond to the physical matrix element only for $x = x_n$. On the other hand the RHS of Eq. (63) provides with an interpolating function for the matrix elements at different x_n , which is independent of the dynamics of the final state ϕ_n . We plot this function in Fig. 5. We can see that the next-to-leading order (NLO) is a correction compared with the leading order (LO), for all values of x and the hard-collinear mass we consider. For instance, if we take $x = 0.5$, we obtain $0.050022 = 0.0470693 + 0.0029527$, where the first term is the LO result and the second one the NLO correction. It should be noticed that most of the contribution to the NLO result comes from the derivative term of the wave-function. We will discuss further this issue in sec. 3.3, when we consider the moments.

So far we have only considered the "diagonal" term of the hadronic matrix element. For the "off-diagonal" term, we are, at present, not able to give approximated analytic results, even in the large n and large m_Q limit. Nevertheless, we have some hints about its analytic form in those limits. They come from two sources: a) the expressions for the moments from the hadronic computation which are already available, for $N = 0, 1$ and 2, within an expansion in $1/m_Q$ [4]; and b) the results from the effective theory with

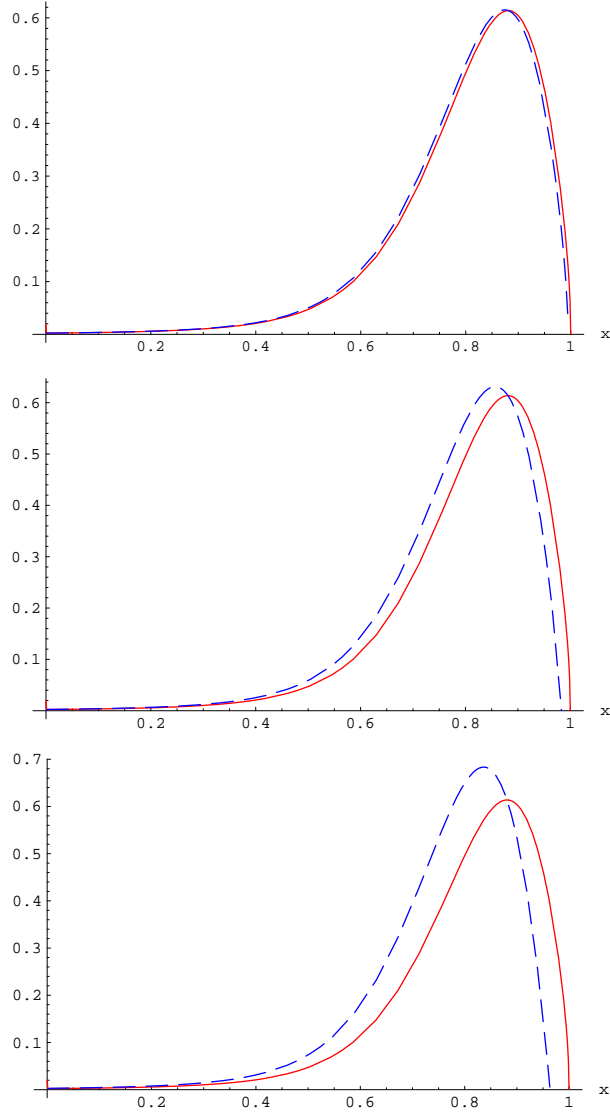


Figure 5: *The solid red line is the LO expression of the RHS of Eq. (63). The dashed blue line is the NLO result. We take $m_Q = 10\beta$ and $m_s = \beta$, whereas $m_c = \beta, 2\beta$ and 3β for the first, second, and third figures, respectively.*

one-loop accuracy. As we will see, to get agreement with these results, the leading term in the large n and large m_Q limit of the "off-diagonal" correction should renormalize the masses of the hard-collinear and heavy quark of the "diagonal" term. In practice, one should have (although the absolute sign cannot be obtained, the relative sign with respect

the "diagonal" term is fixed):

$$\begin{aligned}
& -\beta^2 \frac{1-x}{(P_{H_Q}^+)^2} \sum_{n'=0}^{\infty} (-1)^{n'} \int_0^1 \int_0^1 \int_0^1 dy dt dz \frac{\phi_{n'}^{Qc}(y) \phi_n^{cs}(t) \phi_{n'}^{Qc}(z)}{(t(1-x) + (1-z)x)^2} \\
& \times (\phi_{H_Q}(x + (1-x)t) - \phi_{H_Q}(xz)) \simeq \frac{m_Q}{M_{H_Q}^2} \frac{\phi_{H_Q}(x)}{x} \pi \beta \\
& \times \left(-\frac{\beta^2}{M_{H_Q}^2} \frac{\phi'_{H_Q}(x)}{\phi_{H_Q}(x)} + \frac{1}{x} \frac{\beta^2}{M_{H_Q}^2} - \frac{\beta^2}{2m_Q^2} + \dots \right). \tag{65}
\end{aligned}$$

Although we were not able to check this equation on an analytic basis, we have been able to check it on a numerical basis. We show this comparison in Fig. 6. We can see that the LHS and RHS of Eq. (65) converge to the same value as expected. We have also checked that if we vary the masses⁴, the same pattern survives (as far as the heavy quark mass is large enough). Note that this term is a correction in the $1/m_Q$ expansion.

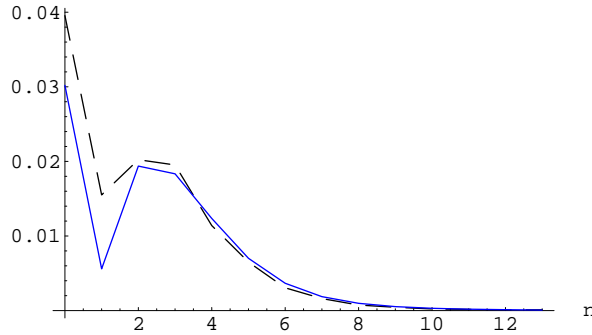


Figure 6: *Plot of the absolute value of the LHS (dashed line) and RHS (solid line) of Eq. (65) for $x = x_n = 1 - M_n^2/M_{H_Q}^2$. To improve the numerical accuracy, we use the difference between the LHS and the first term of the RHS of Eq. (62) for the numerical value of the LHS of Eq. (65). We take the values $m_Q = 10\beta$, $m_c = \beta$ and $m_s = \beta$.*

Overall, we find that the total="diagonal"+"off-diagonal" matrix element can be written in the following way (up to a global sign) for large n and m_Q :

$$\int_0^1 dz \phi_n^{cs}(z) \phi_{H_Q}(z) \simeq \pi \beta \frac{m_{Q,R}}{M_{H_Q}^2} \frac{1}{x} \phi_{H_Q}(x) \left(1 + \frac{m_{c,R}^2}{m_{Q,R}^2} \left(\frac{\phi'_{H_Q}(x)}{\phi_{H_Q}(x)} - \frac{1}{x} \right) \right) \Big|_{x=x_n}. \tag{66}$$

Note that the RHS of Eq. (66) can be understood as a function of x . Strictly speaking this expression is singular for $x \rightarrow 0$. Nevertheless, this effect only shows up for very

⁴One should note though that the computations of the 't Hooft wave function with tachyonic masses are problematic at the numerical level. This problem affects the accuracy of the numerical results and is more acute if one consider the derivate of the wave-function on a point-to-point basis.

small values of x , which are not included in the plots. We can check how well this curve compares with the exact hadronic computation for different values of the hard-collinear and heavy quark masses. We show the results in Figs. 7 and 8. On the one hand we plot the hadronic matrix elements: The LHS of Eq. (62) and the diagonal term of the RHS of Eq. (62). This allows to visualize the difference of working with renormalized and not-renormalized masses (actually the only place where this difference is visible is in the hard-collinear mass multiplying the derivative of the 't Hooft wave function of the H_Q meson). On the other hand we plot the function obtained from the boundary-layer approximation, Eq. (66), for all values of x , also with renormalized and not-renormalized masses. We can see that the agreement between the layer-function and the hadronic result is very good up to very low values of n or, in other words, up to quite near the $x \rightarrow 1$ limit⁵. Our results are also quite good up to relatively low values of the heavy quark mass. We can also see that the dependence on the hard-collinear mass is very well understood with our analytic formula. Moreover, we can also see how the effect of the non-diagonal term of the RHS of Eq. (62) is equivalent to renormalizing the heavy quark and hard-collinear mass in the region where we can trust our results⁶. Overall, we get a very consistent picture.

We find the equality Eq. (66) quite remarkable. It implies that the partial decay width Γ_n becomes independent of the final state wave function properties for higher excitations. The dependence on the final state only appears through $x_n = 1 - M_n^2/M_{H_Q}^2$:

$$\Gamma_n \stackrel{n \rightarrow \infty}{=} \frac{G^2 M_{H_Q}}{4\pi} \frac{m_{Q,R}^2}{M_{H_Q}^2} \frac{\pi^2 \beta^2}{M_{H_Q}^2} \frac{1}{x_n} \phi_{H_Q}^2(x_n) \left[1 + 2 \frac{m_{c,R}^2}{m_Q^2} \left(\frac{\phi'_{H_Q}(x_n)}{\phi_{H_Q}(x_n)} - \frac{1}{x_n} \right) + \dots \right]. \quad (68)$$

The differential decay rate then reads

$$\begin{aligned} \frac{d\Gamma^{(+)}}{dx} &= \frac{1}{2} \sum_{M_n \leq M_{H_Q}} \frac{G^2 M_{H_Q}}{4\pi} \frac{m_{Q,R}^2}{M_{H_Q}^2} \frac{\pi^2 \beta^2}{M_{H_Q}^2} \frac{1}{x_n} \phi_{H_Q}^2(x_n) \\ &\times \left[1 + 2 \frac{m_{c,R}^2}{m_Q^2} \left(\frac{\phi'_{H_Q}(x_n)}{\phi_{H_Q}(x_n)} - \frac{1}{x_n} \right) + \dots \right] \delta \left(x - 1 + \frac{M_n^2}{M_{H_Q}^2} \right). \end{aligned} \quad (69)$$

⁵Actually, the agreement is even too good for the $x \rightarrow 1$ limit, where the layer-function approximation, in principle, does not apply. One could not ruled out this to be a numerical accident. For instance, if we use

$$\int_0^1 dz \phi_n^{cs}(z) \phi_{H_Q}(z) \simeq \pi \beta \frac{m_{Q,R}}{M_{H_Q}^2} \frac{1}{x + \frac{m_{c,R}^2}{m_{Q,R}^2}} \phi_{H_Q} \left(x + \frac{m_{c,R}^2}{m_{Q,R}^2} \right) \Big|_{x=x_n}, \quad (67)$$

instead of Eq. (66), which is also correct to the order of interest, the agreement is less good in the $x \rightarrow 1$ region. On the other hand, Eq. (67) incorporates subleading partial effects which may jeopardize the agreement.

⁶In the effective field theory, this renormalization would be produced by one-loop ($\sim \beta^2$) corrections. We can see that their effects are very tiny for basically all values of x . In the hadronic computation it reflects in the fact that the "off-diagonal" effects are also very small. Actually, the basic effect that it is seen is the renormalization of the hard-collinear mass that appears in the hard-collinear propagator in the effective theory. This is what is to be expected in the SCETI region, in the OPE region the $1/m_Q^2$ corrections are too small to be seen by the eye (unless the hard-collinear mass is large enough).

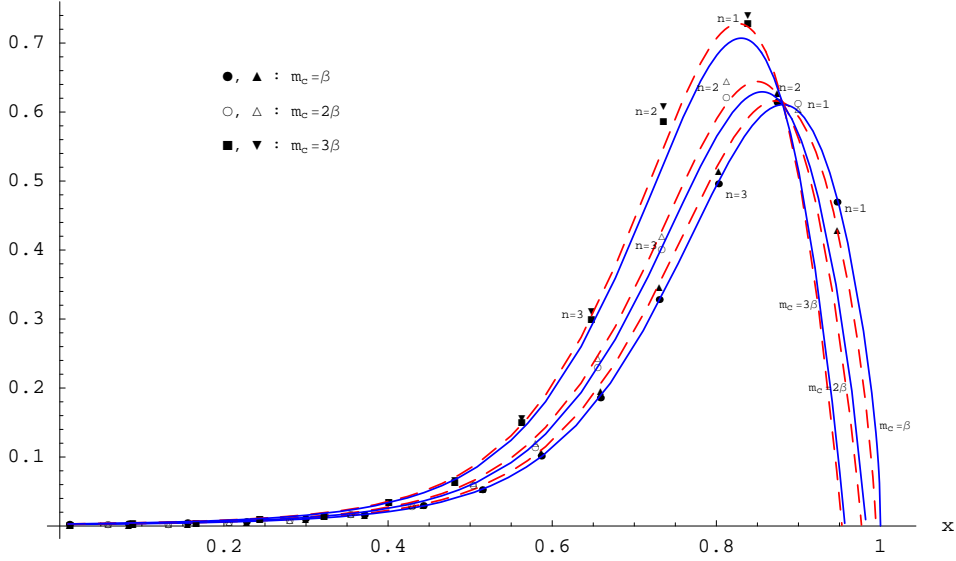


Figure 7: The solid blue lines represent Eq. (66) for values of $m_c = \beta, 2\beta$ and 3β . The dashed red lines represent Eq. (66) for values of $m_c = \beta, 2\beta$ and 3β replacing all the renormalized masses by their bare values: $m_{i,R} \rightarrow m_i$. The dots or squares represent the LHS of Eq. (62) for different values of n . The triangles represent the diagonal term of the RHS of Eq. (62). In both cases the values of m_c are $\beta, 2\beta$ and 3β . We take $m_Q = 10\beta$ and $m_s = \beta$ in all cases.

This expression will be suitable to a smoother connection with the computation using effective field theories.

Eq. (69) applies to the kinematical situation $1 - x \gg \beta^2/m_Q^2$. It includes the leading term in an expansion in $1/m_Q$ and $1/n$. Some kinematical $1/m_Q$ corrections are automatically included by working with the exact ϕ_{H_Q} wave function instead of working with the strict static limit. The corrections of order $m_c^2/m_Q^2, \beta^2/m_Q^2$ have also been included. In principle, this expression could be systematically improved by considering corrections in $1/m_Q$ and $1/n$. Nevertheless, this would require to know the corrections in $1/n$ to the integrals that appear in our expressions, which at present are not known. We expect to study further this issue in the future.

Finally, we would like to stress that the limit $m_c \rightarrow 0$ has to be taken with care, as it is evident from Eq. (62). A naive limit $m_c \rightarrow 0$ may lead to wrong results.

3.3 Moments

The differential decay rate is not a very well defined object in the large N_c , since it becomes either infinity or zero. In particular its comparison with the expressions obtained from effective theories that use perturbative factorization is not possible, as we will see in the

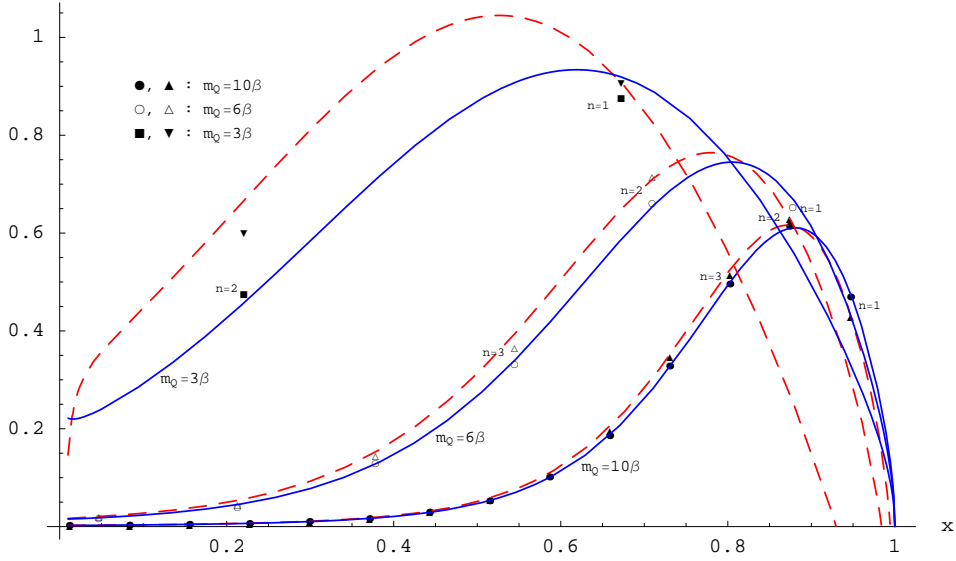


Figure 8: The solid blue lines represent Eq. (66) for values of $m_Q = 10\beta$, 6β and 3β . The dashed red lines represent Eq. (66) for values of $m_Q = 10\beta$, 6β and 3β replacing all the renormalized masses by their bare values: $m_{i,R} \rightarrow m_i$. The squares or dots represent the LHS of Eq. (62) for different values of n . The triangles represent the diagonal term of the RHS of Eq. (62). We take $m_c = \beta$ and $m_s = \beta$ in all cases.

next sections: on the one hand one obtains a series of delta terms, whereas on the other one gets an smooth function of x^7 . At this respect one may think that it is better to work with moments⁸:

$$M_N \equiv \int_0^1 dx x^{N-1} \frac{d\Gamma}{dx}. \quad (70)$$

Exact expressions for the moments in terms of hadronic matrix elements can be ob-

⁷Real experimental data on semileptonic B meson decays is usually available in terms of moments, and therefore so are the corresponding theoretical predictions. In Ref. [27] the differential decay rate itself was reconstructed from available experimental information on its moments, allowing thus for a more general comparison between theory and experiment.

⁸This actually does not cause the problem of quark-hadron duality to vanish, though, as it has been emphasized in Ref. [4] for the inclusive decay width.

tained by using the expressions for $\frac{d\Gamma^{(+)}}{dx}$ or $\frac{d\Gamma^{(-)}}{dx}$ obtained in the previous subsection:

$$M_N = \frac{G^2 M_{H_Q}}{4\pi} \sum_{M_n \leq M_{H_Q}} x_n^N \left| \frac{m_Q m_c}{(P_{H_Q}^+)^2} \int_0^1 dz \frac{\phi_{H_Q}(x_n + (1-x_n)z) \phi_n^{cs}(z)}{(x_n + (1-x_n)z)z} \right. \\ \left. - \beta^2 \frac{1-x_n}{(P_{H_Q}^+)^2} \sum_{n'=0}^{\infty} (-1)^{n'} \int_0^1 \int_0^1 \int_0^1 dy dt dz \frac{\phi_{n'}^{Qc}(y) \phi_n^{cs}(t) \phi_{n'}^{Qc}(z)}{(t(1-x_n) + (1-z)x_n)^2} \right. \\ \left. \times (\phi_{H_Q}(x_n + (1-x_n)t) - \phi_{H_Q}(x_n z)) \right|^2, \quad (71)$$

$$M_N = \frac{G^2 M_{H_Q}}{4\pi} \sum_{M_n \leq M_{H_Q}} x_n^N \left| \int_0^1 dy \phi_n^{cs}(y) \phi_{H_Q}(y) \right|^2, \quad (72)$$

where $x_n = 1 - M_n^2/M_{H_Q}^2$. As we have mentioned previously both expressions for the moments yield the same result.

In order to perform some analytical analysis, it is necessary to be able to compute the different matrix elements or, at least, the sum of matrix elements that contributes to the moments. In general this is not possible. Nevertheless, for some specific cases, it is possible to obtain approximated expressions. If we take M_1 from Eq. (72), it corresponds to the total decay width. In this case it is possible [4] to obtain a closed analytic expression up to $O(1/M_{H_Q}^5)$ suppressed corrections in terms of expectation values of matrix elements of the H_Q -meson wave function by using sum rules:

$$M_1 \equiv \Gamma_{H_Q} = \frac{G^2 (m_Q^2 - m_c^2)}{4\pi M_{H_Q}} \int_0^1 \frac{dx}{x} \phi_{H_Q}^2(x) - \sum_{M_n \geq M_{H_Q}} \Gamma_n \quad (73)$$

$$= \Gamma_Q \left[\frac{m_Q}{M_{H_Q}} \int_0^1 \frac{dx}{x} \phi_{H_Q}^2(x) + O\left(\frac{1}{m_Q^5}\right) \right], \quad (74)$$

where

$$\Gamma_Q = \frac{G^2 m_Q^2 - m_c^2}{4\pi m_Q} \quad (75)$$

is the free heavy quark decay rate, and Γ_n has been defined in Eq. (61) (note that in Eq. (73) they represent partial decay widths that are not allowed by momentum conservation).

For $N \neq 0$, in general, it is not possible to follow the same procedure, since the sum rules become divergent. Only for $N = 0, 2$, it is also possible to obtain a finite result:

$$M_0 = \frac{G^2 M_{H_Q}}{4\pi} \left(1 + O\left(\frac{1}{m_Q^5}\right) \right), \quad (76)$$

$$\begin{aligned}
M_2 &= \frac{G^2 M_{H_Q} (m_Q^2 - m_c^2)^2}{4\pi M_{H_Q}^4} \int_0^1 \frac{dy}{y^2} \phi_{H_Q}^2(y) - \frac{1}{M_{H_Q}^2} \sum_{M_n \geq M_{H_Q}} (M_{H_Q}^2 - M_n^2) \Gamma_n \\
&= \Gamma_Q \left[\frac{m_Q}{M_{H_Q}} \frac{m_Q^2 - m_c^2}{M_{H_Q}^2} \int_0^1 \frac{dx}{x^2} \phi_{H_Q}^2(x) + O\left(\frac{1}{m_Q^3}\right) \right]. \tag{77}
\end{aligned}$$

The $N = 0$ case is basically due to probability conservation. It can be noticed that the above moments can be written in a more compact way in the following form:

$$M_N = \frac{G^2 M_{H_Q}}{4\pi} \left[\left(\frac{m_Q^2 - m_c^2}{M_{H_Q}^2} \right)^N \int_0^1 \frac{dx}{x^N} \phi_{H_Q}^2(x) + O\left(\frac{1}{m_Q^3}\right) \right], \quad \text{for } N = 0, 1, 2. \tag{78}$$

For N larger than two the integral becomes divergent.

The above expressions contain some implicit dependence on the heavy quark mass, since, so far, we have used the exact H_Q -meson wave function. If we perform an explicit expansion in $1/m_Q$, one obtains, up to $O(1/m_Q^3)$,

$$M_0 = \frac{G^2 m_Q}{4\pi} \left[1 + \frac{\langle t \rangle}{m_Q} - \frac{\langle t \rangle^2 - 3\langle t^2 \rangle + \beta^2}{2m_Q^2} + O\left(\frac{1}{m_Q^3}\right) \right], \tag{79}$$

$$M_1 = \frac{G^2 m_Q}{4\pi} \left[1 + \frac{\langle t \rangle^2 - \langle t^2 \rangle + \beta^2 - 2m_c^2}{2m_Q^2} + O\left(\frac{1}{m_Q^3}\right) \right], \tag{80}$$

$$M_2 = \frac{G^2 m_Q}{4\pi} \left[1 - \frac{\langle t \rangle}{m_Q} + \frac{3\langle t \rangle^2 - 3\langle t^2 \rangle + 3\beta^2 - 4m_c^2}{2m_Q^2} + O\left(\frac{1}{m_Q^3}\right) \right], \tag{81}$$

where the static limit expectation values are defined in Eq. (38). We relegate the numerical comparison of these expressions with the exact ones to sec. 5.1, since these expressions will also be obtained from the effective theory computation.

The above expressions for the moments have been obtained for low N . Therefore, they correspond, somewhat, to the kinematical regime where the OPE is valid. We may consider to use the approximated expression obtained using the properties of the final state wave function for large n , i.e. the layer function, for $\frac{d\Gamma^{(+)}}{dx}$ in Eq. (69). Therefore, we expect the expressions that we will obtain to be also valid for larger values of N : $N \leq M_Q/\beta$ ($1 - x \sim \beta/m_Q$), up to corrections of order $N\beta^2/m_Q^2 \sim \beta^2/M_n^2$. This means the kinematical regime where the OPE and SCETI are valid. Note, however, that we integrate for all x in the moments. Therefore, this includes contributions from $x \sim 1$, equivalent to final states with $n \sim 1$ for which the layer-function approximation is not valid. A very rough estimate sets the contribution of these states to the moments (for $N \sim 1$) of $O(1/m_Q^4)$ or smaller. In any case the fact that we have problems to obtain approximate analytic expressions for Eq. (65) sets the accuracy of the calculation. The

expressions that we obtain for the moments read

$$\begin{aligned}
M_N &\simeq \frac{G^2 M_{H_Q} m_{Q,R}^2 \pi^2 \beta^2}{4\pi M_{H_Q}^2 M_{H_Q}^2} \sum_{M_n \leq M_{H_Q}} \int_0^1 dx x^N \frac{\phi_{H_Q}^2(x)}{x} \\
&\times \left[1 + 2 \frac{m_{c,R}^2}{m_Q^2} \left(\frac{\phi'_{H_Q}(x)}{\phi_{H_Q}(x)} - \frac{1}{x} \right) \right] \delta \left(x - 1 + \frac{M_n^2}{M_{H_Q}^2} \right) + \dots \\
&\simeq \frac{G^2 M_{H_Q} m_{Q,R}^2 \pi^2 \beta^2}{4\pi M_{H_Q}^2 M_{H_Q}^2} \sum_{M_n^2 \leq M_{H_Q}^2} \int_0^1 dx x^N \frac{\phi_{H_Q}^2 \left(x + \frac{m_{c,R}^2}{m_{Q,R}^2} \right)}{\left(x + \frac{m_{c,R}^2}{m_{Q,R}^2} \right)^2} \delta \left(x - 1 + \frac{M_n^2}{M_{H_Q}^2} \right) + \dots,
\end{aligned} \tag{82}$$

where in the second equality we have reshuffled the NLO correction to the layer function in a way that is correct at the accuracy of the calculation and that it will ease some intermediate analytic computations, making them more compact.

By working with moments, which imply an integral over all x , it becomes possible to perform a Euler-McLaurin expansion for the sum over n , which, at lowest order, it is just equivalent to replace the sum by an integral: $\sum_n \rightarrow \int dn$. This replacement allows us to make quantitative the comparison between the perturbative and hadronic result. Note however that the Euler-McLaurin expansion is an asymptotic expansion. Therefore, it is a difficult question to assign an error. Here we will not dwell further on the error used by replacing the sum by the integral. To go beyond this approximation would require a better knowledge of the properties of the layer function and a systematic procedure to get corrections from it, which is relegated for future work. In any case, the result we obtain after the smearing reads

$$\begin{aligned}
M_N &= \frac{G^2 M_{H_Q} m_{Q,R}^2}{4\pi M_{H_Q}^2} \int_0^1 dx x^N \frac{\phi_{H_Q}^2 \left(x + \frac{m_{c,R}^2}{m_{Q,R}^2} \right)}{\left(x + \frac{m_{c,R}^2}{m_{Q,R}^2} \right)^2} = \frac{G^2 M_{H_Q} m_{Q,R}^2}{4\pi M_{H_Q}^2} \\
&\times \int_0^1 \left(1 - \frac{m_{c,R}^2}{x m_{Q,R}^2} \right)^N \frac{dx}{x^2} x^N \phi_{H_Q}^2(x) \simeq \frac{G^2 M_{H_Q} m_{Q,R}^2}{4\pi M_{H_Q}^2} \left(1 - \frac{m_{c,R}^2}{m_{Q,R}^2} \right)^N \int_0^1 \frac{dx}{x^2} x^N \phi_{H_Q}^2(x),
\end{aligned} \tag{83}$$

where in the last equality we have used $\frac{m_{c,R}^2}{x m_{Q,R}^2} \simeq \frac{m_{c,R}^2}{m_{Q,R}^2}$, which is correct with the accuracy of our calculation. Eq. (83) is correct at leading order in the OPE and SCETI kinematic region. In the OPE region is correct up to, and including, $O(1/m_Q^2)$ corrections in the situation when it is possible to compare with the already known hadronic results ($N = 0, 1, 2$). Note that in order to get this agreement it is crucial to "renormalize" the masses of the hard-collinear and heavy quark. This renormalization effect can be traced back to the "off-diagonal" contribution to the "-" current. We can also give expressions for a

general N within an expansion in $1/m_Q$. At $O(1/m_Q^2)$ we find the following expression⁹

$$M_N^{OPE} \simeq \frac{G^2 m_Q}{4\pi} \left(1 - (N-1) \frac{\langle t \rangle}{m_Q} + \frac{(2N-1)\beta^2 - 2Nm_c^2}{2m_Q^2} \right. \\ \left. + \frac{(2(N-2)+3)\langle t \rangle^2 + ((N-2)(N-3)-3)\langle t^2 \rangle}{2m_Q^2} + O\left(\frac{1}{m_Q^3}\right) \right). \quad (84)$$

The expression for M_N , Eq. (83), also applies to the SCETI region. As we have already mentioned, the above expression is correct at leading order in the $\beta^2 N/m_Q^2$ expansion. Our expression also includes the subleading corrections of $O(\beta/m_Q)$. Formally, in this kinematical regime we could approximate M_N by the following expression (note that $\phi_Q^2(x)$ should also be expanded in $1/m_Q$)

$$M_N^{SCETI} \simeq \frac{G^2 M_{H_Q}}{4\pi} \frac{m_Q^2}{M_{H_Q}^2} \int_0^1 dx e^{-N(1-x)} \phi_Q^2(x) \\ \times \left(1 + 2(1-x) - N \frac{(1-x)^2}{2} - N \frac{m_{c,R}^2}{m_Q^2} + \dots \right), \quad (85)$$

where the terms neglected are of relative order β^2/m_Q^2 , which, in principle, we cannot claim to have all of them. The reason is that we have not considered terms of the type $\beta^4/m_Q^4 \partial^2 \phi_{H_Q}^2(x)/\partial^2 x$, which would contribute to the moments at NNLO in the SCETI region. Note again the necessity to renormalize the hard-collinear mass. This effect can be traced back to the derivative term in the boundary layer approximation of the "off-diagonal" term and can be unambiguously identified numerically. The reason this term is enhanced is because one has contributions like

$$\int_0^1 dx x^{N-2} \frac{\partial \phi_{H_Q}^2(x)}{\partial x} = -(N-2) \int_0^1 dx x^{N-3} \phi_{H_Q}^2(x). \quad (86)$$

Finally, we would also like to consider another observable that is usually used in the study of the differential heavy meson decay rate. Since, in real life, many times one cannot measure over all the spectrum of final particles, one has to introduce a cutoff to the inclusive measurement. Therefore, the following observable is usually considered:

$$\Gamma_{H_Q}(y) \equiv \frac{1}{\Gamma_{H_Q}} \int_{1-y}^1 dx \frac{d\Gamma}{dx}(x), \quad 0 \leq y \leq 1. \quad (87)$$

We relegate a numerical analysis of this observable as well as of the moments to sec. 5.1.

⁹Quite remarkable, we obtain the same expression if we extrapolate Eq. (78) to values of N different of 0, 1, 2, for which it was originally obtained, and we expand in $(1-x)$ before doing the integral.

SCETI fields	
Hard-collinear light quark	ξ_{hc}
Hard-collinear gluon	A_{hc}^μ
Soft light quark	q_s
Soft gluon	A_s^μ

Table 3: *Relevant fields in SCETI.*

SCETI modes				
Mode	p^-	p_\perp	p^+	p^2
Hard	1	1	1	1
Hard-Collinear	1	λ	λ^2	λ^2
Soft	λ^2	λ^2	λ^2	λ^4

Table 4: *Relevant momentum configurations (modes) in SCETI.*

4 SCETI: Multimode approach

We want to describe now the hadronic results obtained in the previous section using effective field theories. The aim is to describe the decay of the heavy meson to a bunch (one in the large N_c) of hadronic particles with invariant moment $P_X^2 = M_{H_Q}^2(1-x) \gg \Lambda_{\text{QCD}}^2$. The usual procedure, this scale being much larger than Λ_{QCD} , is to use perturbative computations. Actually, here lies the heart of the problem of quark-hadron duality, since we are working in the Minkowskian region and, therefore, near the mass-shell region. Nevertheless, we expect that by working with the 't Hooft model we may better visualize the problem.

In this section we first approach the problem adapting the present formulations of effective theories for very energetic collinear particles [9,10,11,12], in particular of Ref. [11], to the two dimensional case, and we relegate an alternative approach to the next section. In those references, one attempts to explicitly obtain all the modes that one has in the theory from perturbation theory. This heavily relies in the concept of threshold expansion of Feynman diagrams [24].

In this paper we will not exhaustively explore the different modes that may appear in the 't Hooft model. We will see that at the order we will work here it will be enough to work with hard-collinear and soft modes¹⁰, for which we set the notation in Table 3. Our aim is to try to see explicitly at which point in this effective field theory derivation one approximates the hadronic result by a partonic one.

First of all let us set the terminology of the different modes. We have already mentioned that the small expansion parameters are λ and $\bar{\lambda}$. We will formally work in the

¹⁰Nevertheless, we believe the 't Hooft model provides a nice framework on which to explore which modes really appear in SCETI. We expect to pursue this line of research in the future.

situation $\lambda \sim \bar{\lambda} \ll 1$, which corresponds to the SCETI kinematic region. Nevertheless, our results will also be valid in the OPE region where $\bar{\lambda} \sim 1$. In terms of λ , the momenta of the different modes scale as shown in Table 4. The only difference in $D = 1 + 1$ is that there is no perpendicular component p_\perp of the momentum. The momentum is decomposed as

$$p^\mu = n_+ p \frac{n_-^\mu}{2} + p_\perp + n_- p \frac{n_+^\mu}{2}, \quad (88)$$

so that a collinear particle is defined as a particle with large light-cone momentum in the n_+ direction. The fields that are relevant for the effective theory are shown in Table 3. The field of each particle is decomposed into all the possible modes: $\psi = \xi_{hc} + \eta_{hc} + q_s + \dots$. In practice only a few modes contribute to a given field. For instance, the quark s can be approximated by its soft mode: $\psi_s \simeq q_{s,s}$. We also use the notation $p^+ \equiv n_+ p$, and the same for other vector components. A field with momentum p varies in position space according to the uncertainty principle,

$$x^\mu = (x^+, x_\perp, x^-) \sim \left(\frac{1}{p^-}, \frac{1}{p_\perp}, \frac{1}{p^+} \right). \quad (89)$$

The scaling of the quark and gluon fields in D spacetime dimensions can be first naively estimated from the free quark and gluon propagators in position space quantized in the equal-time frame¹¹,

$$\langle 0 | T (\psi(x) \bar{\psi}(y)) | 0 \rangle = \int \frac{d^d p}{(2\pi)^4} \frac{i \not{p}}{p^2 + i\epsilon} e^{-ip \cdot (x-y)}, \quad (90)$$

$$\langle 0 | T (A^\mu(x) A^\nu(y)) | 0 \rangle = \int \frac{d^d p}{(2\pi)^4} \frac{i}{p^2 + i\epsilon} \left[-g^{\mu\nu} + (1 - \alpha) \frac{p^\mu p^\nu}{p^2} \right] e^{-ip \cdot (x-y)}, \quad (91)$$

where the gluon propagator is obtained in a general covariant gauge. Using these propagators, the scaling of the different fields of the effective theory is the following:

- Soft light quark $q_s \sim \lambda^{D-1}$
- Soft gluon $A_s \sim \lambda^{D-2}$
- Hard-collinear gluon $A_{hc}^+ \sim \lambda^{(D-4)/2}$, $A_{hc}^\perp \sim \lambda^{(D-2)/2}$, $A_{hc}^- \sim \lambda^{D/2}$
- Hard-collinear quark $\xi_{hc} \sim \lambda^{(D-2)/2}$, $\eta_{hc} \sim \lambda^{D/2}$

To obtain the scaling of the hard-collinear quark fields, we have decomposed these fields using projection operators

$$\psi_{hc}(x) = \xi_{hc}(x) + \eta_{hc}(x), \quad \xi_{hc}(x) \equiv \Lambda_- \psi_{hc}(x), \quad \eta_{hc}(x) \equiv \Lambda_+ \psi_{hc}(x). \quad (92)$$

¹¹In the light-cone quantization frame things are more complicated, in particular for the fermions, which have different free propagators.

Scaling of the SCETI fields		
Field	$D = 4 [g \sim \lambda^0]$	$D = 2 [g \sim \lambda^2]$
ξ_{hc}	λ	λ^0
η_{hc}	λ^2	λ
gA_{hc}^-	λ^0	λ
gA_{hc}^+	λ	-
gA_{hc}^+	λ^2	λ^3
q_s	λ^3	λ^1
gA_s^μ	λ^2	λ^2

Table 5: *Scaling of the effective theory fields in $D = 4$ and $D = 2$ taking into account the scaling of the coupling.*

Scaling of the integration element	
Fields	d^2x
hc	λ^{-2}
s	λ^{-4}
hc+s	λ^{-2}

Table 6: *Scaling of the integration element in the effective action.*

One can check that for $D = 4$ one recovers the usual scalings of the effective theory. The scalings of the effective theory fields in $D = 4$ and $D = 2$ can be seen in Table 5. One can observe that in $D = 2$ the hard-collinear gluons have negative scalings. The solution to this problem comes by realizing that in $D = 2$ the strong coupling g has dimensions of mass and, actually, sets the scale of Λ_{QCD} so

$$g \sim \lambda^2, \quad (93)$$

and we can see that the scaling of the hard collinear gluons times g is positive.

It can be observed that the hard-collinear gluon field times g does not scale as the corresponding hard-collinear momentum but rather, it is suppressed by powers of λ . This will lead to the result that hard-collinear interactions are suppressed with respect to the corresponding kinetic terms.

A crucial point to fix the scaling of each term in the effective action is to know the scaling of the integration element d^2x , which depends on the fields present on each term. The different scalings can be seen in Table 6.

We are now in the position to write the effective Lagrangian, which we do in the next section.

4.1 Lagrangian and heavy-to-light current

We first want to translate to two dimensions the standard procedure to obtain the effective Lagrangian. This first means to integrate out the η_{hc} component of the hard-collinear field¹². We will only consider the leading order Lagrangian here.

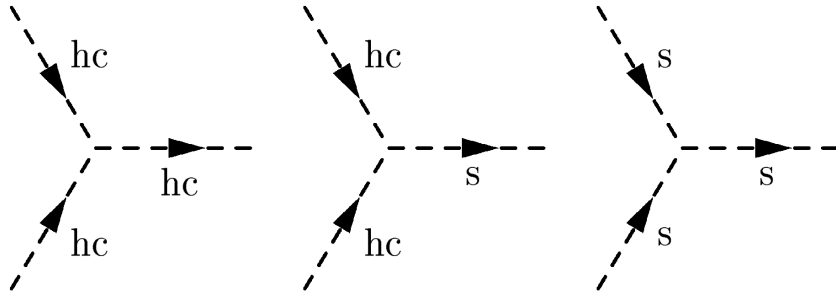


Figure 9: *Allowed vertices by momentum conservation in a theory with only hard-collinear and soft modes. Dashed lines can be either quarks or gluons*

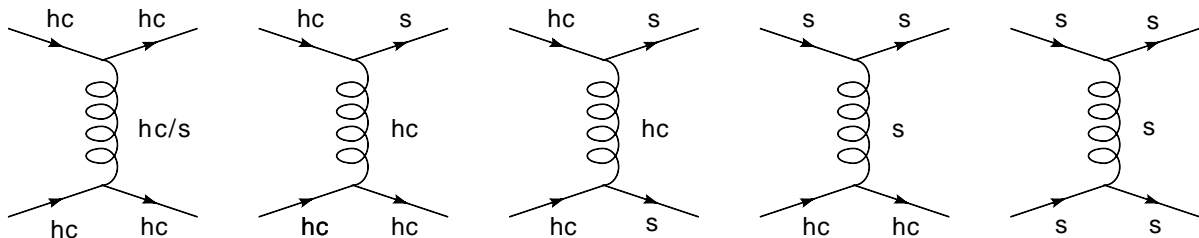


Figure 10: *Allowed scattering processes.*

The allowed vertices by momentum conservation are drawn in Fig. 9. Since the gluons do not appear as physical particles, we are always faced with diagrams of the sort of those shown in Fig. 10. By power counting we can easily see that the self interactions between hard-collinears (in particular those including hard-collinear gluons) are suppressed by powers of λ . Therefore, at leading order, we only have to consider soft gluons and quarks and hard-collinear quarks. The leading order Lagrangian then reads

$$\mathcal{L}^{(0)} = \mathcal{L}_s^{(0)} + \mathcal{L}_{hc}^{(0)} , \quad (94)$$

$$\mathcal{L}_s^{(0)} \equiv -\frac{1}{2} \text{tr} [F_{\mu\nu,s} F^{\mu\nu,s}] + \bar{q}_{s,s} i \not{D}_s q_{s,s} + \mathcal{L}_{HQET} , \quad (95)$$

¹²This could be considered somewhat strange. If we were working in the light-front Hamiltonian frame with light-cone gauge $A^+ = 0$, η_{hc} would correspond to the physical component, $\psi_{hc,+}$, of the field. Therefore, we would be integrating out the physical component of the field and keeping the constraint.

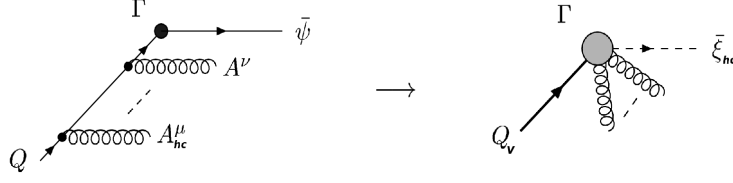


Figure 11: *Tree-level matching of the heavy quark current.*

$$\mathcal{L}_{hc}^{(0)} = \frac{1}{4} \text{tr} [(D_S^+ A_{hc}^- - \partial^- A_{hc}^+)^2] + \bar{\xi}_{c,hc} \left(in_+ D_s - \frac{m_c^2 - i\epsilon}{i\partial^-} \right) \frac{\not{n}_-}{2} \xi_{c,hc} . \quad (96)$$

In this expression we have kept kinematical subleading corrections proportional to the mass of the hard-collinear.

We do not explicitly write the HQET sector of the theory. In practice it will turn out more convenient to implicitly keep the heavy quark mass dependence and to expand at the end of the calculation.

The next step in order to apply SCET1 to the semileptonic decay is to write the heavy-to-light current $\bar{\psi}_c \Gamma Q$ (where $\Gamma = \gamma^\mu$ in our case) in terms of the effective theory fields. The emission of a hard-collinear quark (see Fig. 11) by the near on-shell heavy quark puts it off shell, and it stays off-shell when subsequent hard-collinear and soft gluons are emitted. Therefore the effective current must reproduce these diagrams that are absent in the effective theory, and it can be shown that

$$J_{QCD} = \bar{\psi}_c \Gamma Q = e^{-im_Q vx} \bar{\psi}_c \Gamma \left(1 - \frac{1}{i\cancel{D} - m_Q(1-\not{v})} g\cancel{A}_{hc} \right) Q_v . \quad (97)$$

We must expand the above expression in powers of λ . Starting from

$$Q \equiv \left(1 - \frac{1}{i\cancel{D} - m_Q(1-\not{v})} g\cancel{A}_{hc} \right) Q_v , \quad (98)$$

and defining

$$S_0 \equiv \frac{1}{[i\partial_+ \frac{\not{n}_-}{2} - m_Q(1-\not{v})]} = \frac{1}{v_-} \left(\frac{\not{n}_-}{2m_Q} + \frac{1+\not{v}}{i\partial_+} \right) \sim \lambda^0 , \quad (99)$$

where the scaling is like this because the momentum in the covariant derivative is hard-collinear, since it is the momentum that flows through the heavy quark line once the hard-collinear gluon has been emitted. Expanding in λ , one arrives to the following result

$$Q = \left(1 - S_0 g A_{hc+} \frac{\not{n}_-}{2} + S_0 g A_{hc+} \frac{\not{n}_-}{2} S_0 g A_{hc+} \frac{\not{n}_-}{2} + \mathcal{O}(\lambda^3) \right) (1 + \mathcal{O}(\lambda)) Q_v . \quad (100)$$

In the last term the $\mathcal{O}(\lambda)$ indicates possible contributions coming from the integration of the short component of the heavy quark field.

We would like here to stress the difference with the situation in 4 dimensions, where a hard-collinear Wilson line appears multiplying the effective current. Actually here this also happens but the exponent is suppressed by powers of λ (in four dimensions it is only suppressed by powers of α_s).

This is the first part of the construction of the effective current. The second part consists on the matching of the light quark field ψ_c in terms of the effective theory fields. Since the effective current must be constructed such that it reproduces the on-shell matrix elements with a current insertion of full QCD, we must add the following interaction term

$$\mathcal{L}_j = e^{imvx} \bar{\psi}_c \Gamma \mathcal{Q} B \equiv (\xi_{c,hc}^\dagger + \eta_{c,hc}^\dagger + q_{c,s}^\dagger) j, \quad j \equiv e^{imQvx} \gamma^0 \Gamma \mathcal{Q} B, \quad (101)$$

where $B = -G/\sqrt{2} \bar{l}_a \gamma_\mu l_b$ in our case, to the Lagrangian Eq. (94), and perform again the relevant manipulations (integrating out the small component field η_{hc} and multipole expand), taking now into account the presence of the source term. Now the equations of motion lead to

$$\eta_{c,hc} = \frac{1}{iD_+} [gA_{hc+} q_{c,s} - j], \quad (102)$$

and inserting this in the effective Lagrangian results in the following modified source term

$$\mathcal{L}_j = \left(\xi_{c,hc}^\dagger + q_{c,s}^\dagger + q_{c,s}^\dagger gA_{hc+} \frac{1}{iD^-} \right) j, \quad (103)$$

where the derivative in the last term is hard-collinear and acts to the left. Therefore the full QCD light quark is matched in the effective theory into

$$\psi^\dagger \rightarrow \xi_{c,hc}^\dagger + q_{c,s}^\dagger + q_{c,s}^\dagger gA_{hc+} \frac{1}{iD^-}. \quad (104)$$

Putting everything together results in the following current

$$J_{QCD}(x) = e^{-imQvx} [\mathcal{O}_0 + \mathcal{O}_1 + \dots], \quad (105)$$

where the terms are labeled with their relevant order with respect to the dominant term, which reads

$$\mathcal{O}_0 = \xi_{c,hc}^\dagger \gamma^0 \Gamma Q_v. \quad (106)$$

Note that we have neglected the term $q_{c,s}^\dagger \Gamma Q_v$, since by our kinematical assumptions, there is large momentum transfer to the final state, so the operators of the effective current must contain at least one hard-collinear field to contribute to such final states. The scaling of each term is $\mathcal{O}_0 \sim \lambda$ and $\mathcal{O}_1 \sim \lambda^2$. The final conclusion is that up to gauge invariance subtleties, the heavy-to-light QCD current is simply matched to

$$J_{QCD}(x) \rightarrow e^{-imQvx} \xi_{c,hc}^\dagger \gamma^0 \Gamma Q_v \equiv e^{-imQvx} \mathcal{O}_0, \quad (107)$$

at tree level. This is the result that we need to study factorization in heavy-to-light decays at leading order. Hard fluctuations would be included in the Wilson coefficients C_k of the

operators in the effective current and can be determined by matching calculations so that the general structure of the current reads

$$J_{QCD}(x) = e^{-im_Q vx} \sum_k C_k(m_Q) \mathcal{O}_k . \quad (108)$$

Using field redefinitions, one can see that in SCETI in D=4 at leading power the hard-collinear and soft degrees of freedom decouple [10]. In D=1+1 the same appears to be true. The starting point is Eq. (94). One can see now that redefining the hard-collinear field $\xi_{c,hc}$ using a soft Wilson line,

$$\xi_{c,hc}(x) \equiv Y_s(x) \xi_{c,hc}^{(0)}(x) , \quad (109)$$

$$Y_s(x) \equiv P \exp \left(-ig \int_0^\infty ds A_{s-}(x_- + sn_-) \right) , \quad (110)$$

and redefining the hard-collinear gluons in the following way:

$$A_{hc}^\mu(x) \equiv Y_s(x) A_{hc}^{(0)\mu} Y_s^\dagger(x) , \quad (111)$$

leads to factorization of hard-collinear and soft modes at leading order in the effective Lagrangian,

$$\mathcal{L}^{(0)} = \bar{\psi}_s i \not{D}_s \psi_s + \xi_{c,hc}^{(0)\dagger} \left(i\partial^+ - \frac{m_c^2 - i\epsilon}{i\partial^-} \right) \xi_{c,hc}^{(0)} + \frac{1}{4} \text{tr} \left[(\partial^+ A_{hc}^{(0)-} - \partial^- A_{hc}^{(0)+})^2 \right] . \quad (112)$$

The factorization at the level of hard-collinear fields is somewhat academic at this stage, since they are not going to appear at leading order in the semileptonic decay of the heavy meson. Now all the soft-hard collinear dynamics are encoded in the effective current, that at leading order becomes

$$\mathcal{O}_0 = \xi_{c,hc}^{(0)\dagger} Y_s^\dagger \gamma^0 \Gamma Q_v . \quad (113)$$

In the following subsection we analyze the semileptonic decay using SCETI.

4.2 Semileptonic differential decay rate

In this section we show how factorization can be implemented in this process using SCETI. In sec. 3 we have already written the differential decay rate in terms of the imaginary part of T^{--} . We can now write this hadronic correlator in terms of the SCETI fields. The first step consists on the factorization of the hard modes. We have seen that the QCD current can be expanded in a series of operators in the effective theory. Then the hadronic tensor can be written as

$$T^{--} \equiv i \int d^2x e^{i(-q+m_Q v)x} \sum_{k=k'+k''} H_k(m_Q) \left\langle H_Q | T \{ \mathcal{O}_{k'}^\dagger(x) \mathcal{O}_{k''}(0) \} | H_Q \right\rangle \equiv \sum_k H_k(m_Q) T_{k,eff}^{--} , \quad (114)$$

where the effective hadronic tensor at leading order is given by

$$T_{0,eff}^{--} = i \int d^2x e^{i(-q+m_Qv)x} \langle H_Q | T \{ (\bar{\xi}_{c,hc} \gamma^- Q_v)^\dagger(x) (\bar{\xi}_{c,hc} \gamma^- Q_v)(0) \} | H_Q \rangle . \quad (115)$$

After performing the field redefinitions shown in Eq. (109) the effective tensor reads

$$\begin{aligned} T_{0,eff}^{--} &= i \int d^2x e^{i(-q+m_Qv)x} \langle H_Q | T \{ Q_{v,\alpha}^\dagger(x) Y(x) Y^\dagger(0) Q_{v,\beta}(0) \} | H_Q \rangle \\ &\quad \times \langle 0 | T \{ (\gamma^- \xi_{c,hc})_\alpha(x) (\bar{\xi}_{c,hc} \gamma^-)_\beta(0) \} | 0 \rangle , \end{aligned} \quad (116)$$

where we have used the factorization that the (redefined) soft and hard-collinear modes hold at leading order at the Lagrangian level. Therefore the correlator can be understood as the convolution of the soft and jet function. The heavy quark correlator is explicitly soft gauge invariant due to the Y string. So far the computation has been pretty much similar to the one in four dimensions (in the four-dimensional case there are also hard-collinear strings that here have already been approximated to 1).

Let us now discuss the jet function. We define

$$\langle 0 | T \{ (\gamma^- \xi_{c,hc})_\alpha(x) (\bar{\xi}_{c,hc} \gamma^-)_\beta(0) \} | 0 \rangle \equiv i \int \frac{d^2k}{2\pi} e^{-ikx} J^-(k) , \quad (117)$$

where α and β are Dirac indexes. So far we have not specified the quantization frame. If we quantize in the equal-time frame we obtain at tree level

$$J^- = 2\gamma^- \frac{1}{k^+ - \frac{m_c^2 - i\epsilon}{k^-}} \equiv \gamma^- \tilde{J}^- . \quad (118)$$

If we quantize in the light-front frame with our standard gauge fixing prescription $A^+ = 0$, the $\xi_{c,hc}$ field becomes a constraint (the factor $\frac{m_c^2}{k^-} \sim \frac{m_c^2}{m_Q}$ is treated as a correction when quantizing for consistency). Either way, the imaginary term (the one that appears in the decay rate) reads (to be kept in mind that $k^- \sim m_Q > 0$):

$$Im J^- = -2\pi \gamma^- \delta(k^+ - m_c^2/k^-) . \quad (119)$$

The soft function correlator reads

$$\left\langle H_Q | Q_v^\dagger \gamma^-(x^-) P[\exp(ig \int_0^{x^-} dz^- A^+(z^-))] Q_v(0) | H_Q \right\rangle \equiv 2 \int dp^+ e^{ip^+x^-} S^-(p^+) , \quad (120)$$

where S^- is usually named the shape function.

We are now in position of writing $d\Gamma^{(-)}/dx$ in terms of S^- . We obtain

$$\begin{aligned} \frac{d\Gamma^{(-)}}{dx} &= -\frac{1}{M_{H_Q}} \frac{1}{2(2\pi)x} \frac{G^2}{2\pi} (M_{H_Q}x)^2 \\ &\quad \times \int d^2x e^{-i\frac{q^+x^-}{2}} e^{im_Qvx} \int dp^+ e^{i\frac{p^+x^-}{2}} S^-(p^+) \int \frac{d^2k}{(2\pi)2} e^{-ikx} Im \tilde{J}^- . \end{aligned} \quad (121)$$

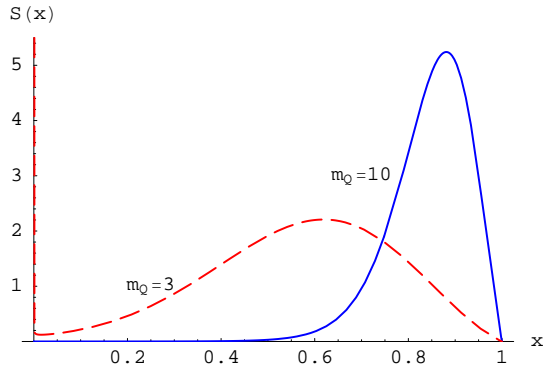


Figure 12: Plot of the shape function with $x = p^+/P_{H_Q}^+$ for the values $m_s = \beta$ and $m_Q = 10\beta$ (solid line) and $m_s = \beta$ and $m_Q = 3\beta$ (dashed line). Strictly speaking the shape function is singular for $x \rightarrow 0$. Nevertheless, this can only be seen by the eye for low values of m_Q .

By doing the x^+ integration and using the fact that the x^+ variations of the Q_v field are small in comparison with m_Q (already used in the above expression), one can set $k^- = m_Q$ in $Im\tilde{J}^-$, which is correct at leading order in the $1/m_Q$ expansion.

At this stage there is a strong simplification if we work in the light-front presented in sec. 2 with gauge fixing $A^+ = 0$, since this allows us to write the shape function in terms of the H_Q -meson wave function squared, which now reads ($p^+ + m_Q v^+ = x M_{H_Q}$)

$$S^-(p^+) = \frac{m_Q^2}{M_{H_Q}^2} \frac{\phi_{H_Q}^2(x)}{x^2} \simeq \frac{m_Q^2}{M_{H_Q}^2} \phi_{H_Q}^2(x). \quad (122)$$

Note that we can do that because the shape function is computed at "equal" times (i.e. for " $x^+ = \text{constant}$ ") and we can use the free expressions for the heavy quark fields. In the last equality we have used the fact that terms of order $1-x$ go like β/m_Q (at least when we compute moments). We show how the shape function looks like in Fig. 12. It is remarkable how similar it is to what one would expect in four dimensions.

Actually one could do a similar analysis in four dimensions as far as one neglects higher Fock components of the H_Q meson state. In this approximation one could relate the shape function with the square of the H_Q wave function and see what is the impact, for instance, in the analysis of Ref. [25].

We could also play the same game for $d\Gamma^{(+)}/dx$. We should then redo the construction of the effective theory, since the hard-collinear quark would actually go in the opposite direction. Everything would work analogously changing J^- and S^- by J^+ and S^+ . J^+ reads equal to J^- changing $\gamma^- \rightarrow \gamma^+$ and $k^+ \leftrightarrow k^-$. Therefore $Im\tilde{J}^+$ and $Im\tilde{J}^-$ produce the same delta function (as far as the x variable is concerned). The definition of S^+ would come from Eq. (120), changing $\gamma^- \rightarrow \gamma^+$ and $x^+ \leftrightarrow x^-$. This has consequences when working in the light-front frame. If we work in the gauge $A^+ = 0$ everything is completely analogous to the computation of $d\Gamma^{(-)}/dx$, changing $+ \leftrightarrow -$ everywhere. In particular

this implies that $S^- = S^+$. It is more interesting to consider our standard gauge fixing $A^+ = 0$. In this situation the hard-collinear field is not a constraint anymore, but the price to pay is that S^+ cannot be easily computed because the fields act at different times. Therefore, it is welcome that we can obtain S^+ from parity arguments.

Our final results for $\text{Im}T$ and $\frac{d\Gamma}{dx}$ read

$$\text{Im}T^{(tree\ level)} = \pi m_Q^2 \phi_{H_Q}^2 \left(x + \frac{m_c^2}{m_Q^2} \right) \frac{1}{M_{H_Q}^2 \left(x + \frac{m_c^2}{m_Q^2} \right)^2}, \quad (123)$$

$$\begin{aligned} \frac{d\Gamma^{(tree\ level)}}{dx} &= \frac{1}{M_{H_Q}} \frac{1}{2(2\pi)x} \frac{G^2}{2\pi} (M_{H_Q}x)^2 2\text{Im}T^{(tree\ level)} \\ &= \frac{G^2 M_{H_Q}}{4\pi} \left(\frac{m_Q}{M_{H_Q}} \right)^2 \frac{1}{\left(x + \frac{m_c^2}{m_Q^2} \right)^2} \phi_{H_Q}^2 \left(x + \frac{m_c^2}{m_Q^2} \right), \end{aligned} \quad (124)$$

where in both expressions, we have included the subleading kinematical corrections, and those due to the mass of the hard-collinear, which are also parametrically subleading.

The moments then read

$$M_N^{(tree\ level)} = \frac{G^2 M_{H_Q}}{4\pi} \frac{m_Q^2}{M_{H_Q}^2} \left(\frac{m_Q^2 - m_c^2}{m_Q^2} \right)^N \int_0^1 dx x^{N-2} \phi_{H_Q}^2(x). \quad (125)$$

We first note that this expression agrees with the result shown in Eq. (83) at LO in $1/m_Q$. The $O(m_c^2/m_Q^2)$ corrections are also correctly incorporated. The first discrepancies are of $O(\beta^2/m_Q^2)$. We need a one-loop analysis to incorporate them, which we postpone to the next section.

Finally, we would like to emphasize that the effective field theory computation has lost the information of the final bound state. This can be visualized by comparing Eq. (124) with the exact hadronic expressions, which consist of a discrete sum over resonances.

5 Soft-(Collinear) Effective Theory in $D = 1 + 1$

In the previous section we have worked out SCET1 and the differential decay rate at leading order in λ . The procedure seems to be quite cumbersome. In principle, it could be possible to extend the previous analysis to higher orders in λ . Nevertheless, the process becomes tedious and, in principle, other modes should be included in the theory. This approach does not explicitly profit from the fact that hard-collinear modes appear from a very specific interaction (the weak one) and that the interaction takes place at very short "times" in the x^+ axis. Instead we will follow here an alternative approach and we will derive the effective theory by integrating out any (light) particle with $P^- \sim m_Q$. This will make the effective field theory non-hermitian, introducing imaginary terms in

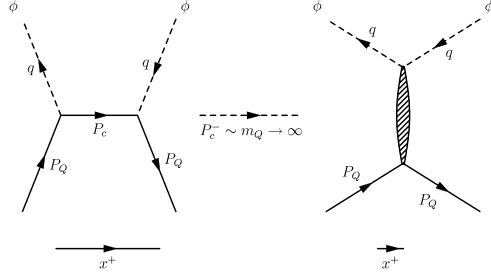


Figure 13: *Symbolic plot to represent the matching from QCD to the effective theory of the (tree-level) diagram, the imaginary part of which produces the decay of the heavy quark to a hard-collinear quark and the ϕ particle. The RHS of the figure represents the effective vertex in the effective theory. The shape of the effective vertex represents that it is local in x^+ but not in x^- .*

the Lagrangian. This should not be considered unusual since this also happens for non-relativistic effective theories. The idea, which we have already mentioned previously, is that diagrams for which the P^- momentum flow are of the order of m_Q are local with respect to the x^+ axis in the light-cone frame and, once we have chosen the quantization frame to be $x^+ = \text{constant}$, we can construct the corresponding effective Hamiltonian. Therefore, the effects due to the hard-collinear fields can effectively be reproduced in the effective theory by a local vertex in x^+ although not local in the other components (see Fig. 13). We should stress that at the end of the day we only want to describe the differential decay rate at leading order in the weak interactions. Therefore, they can be described by a purely imaginary vertex interaction.

The effective degrees of freedom of our theory will be only soft ones (at least to the order to which we will work here). This considerably simplifies our approach compared with others where the derivation of the effective theory is performed investigating all possible modes existing in the theory. Actually one should not call this effective theory "soft-collinear", since the collinear modes do not appear in the theory anymore, rather one may call it HQET but with some non-hermitian terms.

The fact that our interactions will be almost local in x^+ -times will also have important consequences in how the computation is performed. In principle, once all the dependence in P_X^- has disappeared from the interaction¹³, the interaction only depends on P_Q^+ and q^+ . This means that one can use the free-field expressions for the fields in the effective interaction. Note that this is so even if the momentum P_X^+ flowing in the diagram is small. We also have to take into account that we know the explicit expressions of the bound states in terms of the free-field expressions of the field. Therefore, we will be able

¹³More precisely, one can replace P_X^- and P_X^+ by a function of m_Q , P_Q^+ and q^+ using the equations of motion up to residual x^+ "time-dependent" terms, which can be expanded in an expansion in $1/m_Q$. One could get rid of these time-dependent terms systematically using field redefinitions. Nevertheless, in this paper, we do not reach enough precision to worry about this problem.

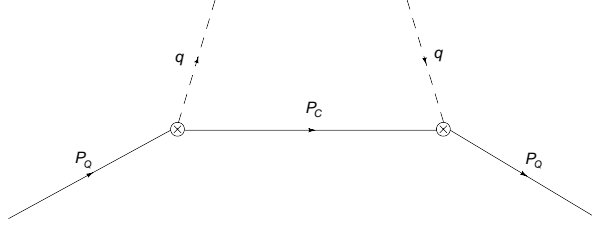


Figure 14: *Tree level diagram, the imaginary part of which gives the leading contribution to the effective vertex in the effective theory, Eq. (129).*

to obtain explicit expressions of the matrix elements in terms of the 't Hooft wave function of the bound states, once we project the effective interaction to the physical states. It is then when the non-perturbative dynamics appears.

An important point here is that the effective vertex can be obtained using perturbation theory, order by order in β^2 . Since β^2 has dimensions in two dimensions, the inclusion of β^2 terms produces subleading effects in the OPE. This is so because, even if $P_X^+ \sim \beta$, P_X^+ typically appears in the combination (except for the leading term) β^2/P_X^2 , which could be interpreted as $\sim \beta^2/M_n^2$. Therefore, if we restrict ourselves to the kinematical situation $P_X^2 \gg \beta^2$, the effective interaction can be obtained using perturbation theory. This is what we will do in what follows.

Our starting point is the Lagrangian of QCD where the gluons and the ψ_- component have been integrated out, i.e. Eq. (4), coupled to the electroweak effective vertex (41). We then want to integrate out any (light) degree of freedom with $P^- \sim m_Q$ and build an effective theory with only soft (light and heavy) quarks. Then we match the effective theory onto QCD.

At tree level we only have to compute one diagram, which we have to match onto the effective vertex (note that throughout we only demand the imaginary piece to be equal). This is symbolically displayed in Fig. 14.

So far we have not specified neither the gauge nor the quantization frame. For the gauge fixing we follow our standard prescription of $A^+ = 0$. Following the notation of the previous section, at lowest order, the intermediate hard-collinear field becomes a free particle and its propagator reads ($k_{on}^- = m^2/k^+$, $k_{on}^+ = k^+$)

$$\begin{aligned}
 J^- &= \gamma^- \frac{\not{k}_{on} + m}{k^2 - m^2 + i\epsilon} \gamma^- = \gamma^- \left(\frac{\gamma^+ k_{on}^-}{2} + \frac{\gamma^- k^+}{2} + m \right) \gamma^- \frac{1}{k^2 - m^2 + i\epsilon} \quad (126) \\
 &= 2\gamma^- \frac{m^2}{k^2} \frac{1}{k^+ - \frac{m^2 - i\epsilon}{k^-}} \equiv \gamma^- \tilde{J}^-,
 \end{aligned}$$

if we quantize in the light-front frame, and

$$J^- = \gamma^- \frac{\not{k} + m}{k^2 - m^2 + i\epsilon} \gamma^- = 2\gamma^- \frac{1}{k^+ - \frac{m^2 - i\epsilon}{k^-}}, \quad (127)$$

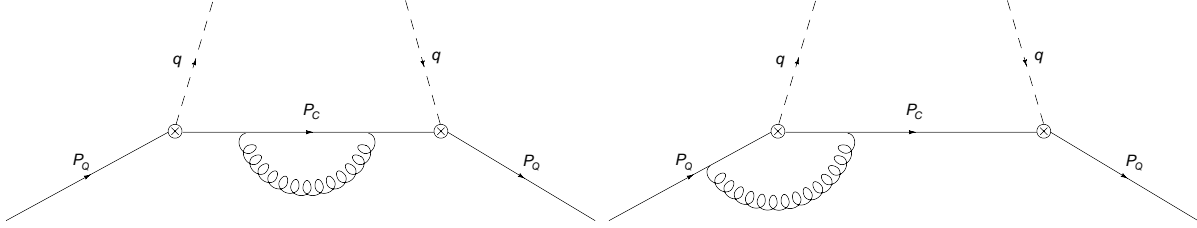


Figure 15: *One loop diagrams (plus their symmetric), the imaginary part of which contribute to the effective vertex in Eq. (130).*

if we quantize in the equal-time frame. We note that the the imaginary term (the one that appears in the decay rate) is equal in the light-front or equal-time quantization frame (to be kept in mind that $k^- \sim m_Q > 0$):

$$ImJ^- = -2\pi\gamma^- \delta(k^+ - m_q^2/k^-). \quad (128)$$

Putting everything together, the contribution to the vertex reads (where we have used the free equation of motion $k^- = P_Q^- = m_Q^2/P_Q^+$)

$$\text{effective vertex} \sim \text{Im} \left[\frac{m_c^2}{P_c^2} \frac{m_Q^2}{(P_Q^+)^2} \frac{1}{P_c^+ - \frac{m_c^2 - i\epsilon}{m_Q^2} P_Q^+} \right]. \quad (129)$$

At $O(\beta^2)$, the following diagrams have to be considered (Fig. 15). Their net effect is to renormalize the masses of the hard collinear and heavy quark. The first diagram renormalizes the hard-collinear mass that appears in the hard-collinear propagator. The effect of the second diagram is to renormalize the masses of the vertex. To simplify the expression we keep subleading terms in the $1/m_Q$ expansion.

By adding all the terms, the effective interaction can be written as ($P_c^+ = P_Q^+ - q^+$)

$$\begin{aligned} \text{effective vertex} &\sim \text{Im} \left[\frac{m_{c,R}^2}{P_c^2} \frac{m_{Q,R}^2}{(P_Q^+)^2} \frac{1}{P_c^+ - \frac{m_{c,R}^2 - i\epsilon}{m_{Q,R}^2} P_Q^+} \right] \\ &= -\pi \frac{m_{Q,R}^2}{(P_Q^+)^2} \delta \left(\left(1 - \frac{m_{c,R}^2}{m_{Q,R}^2} \right) P_Q^+ - q^+ \right), \end{aligned} \quad (130)$$

where with the precision of the calculation, we have replaced m_Q^2 by $m_{Q,R}^2$ within the delta.

We are now in the position to write the effective Lagrangian, which, in fact, is the HQET Lagrangian adding the effective vertex.

$$\mathcal{L} = \mathcal{L}_{HQET} + Im[\mathcal{L}_I] \quad (131)$$

and the effective vertex reads

$$\mathcal{L}_I = -\frac{G^2}{2\pi}(\partial^+\phi) \left(\frac{m_{Q,R}}{i\partial^+}Q_+\right)^\dagger \frac{1}{i\partial^+ - \frac{m_{c,R}^2 - i\epsilon}{m_{Q,R}^2}i\partial^+} \left(\frac{m_{Q,R}}{i\partial^+}Q_+\right) (\partial^+\phi^\dagger). \quad (132)$$

In order to keep the expression for the effective vertex more compact, we have written it in terms of the field Q_+ , had we written it in terms of Q_{+v} , there would be a shift in the derivatives (for instance $i\partial^+ \rightarrow m_Q v^+ + i\partial^+$). We note that the Lagrangian is local in x^+ .

5.1 Semileptonic differential decay rate

At this stage we can compute the semileptonic decay. Actually we will have to compute the imaginary part produced by the effective vertex (132):

$$\text{Im}T_{eff} = \pi m_{Q,R}^2 \phi_{H_Q}^2 \left(\frac{x}{1 - \frac{m_{c,R}^2}{m_{Q,R}^2}}\right) \frac{1}{(M_{H_Q}x)^2} \left(1 - \frac{m_{c,R}^2}{m_{Q,R}^2}\right). \quad (133)$$

The differential decay rate then reads

$$\begin{aligned} \frac{d\Gamma^{pert}}{dx} &= \frac{1}{M_{H_Q}} \frac{1}{2(2\pi)x} \frac{G^2}{2\pi} (M_{H_Q}x)^2 2\text{Im}T_{eff} \\ &= \frac{G^2 M_{H_Q}}{4\pi} \frac{m_{Q,R}^2 - m_{c,R}^2}{m_{Q,R}^2} \left(\frac{m_{Q,R}^2}{M_{H_Q}^2}\right) \frac{1}{x} \phi_{H_Q}^2 \left(\frac{x}{1 - \frac{m_{c,R}^2}{m_{Q,R}^2}}\right). \end{aligned} \quad (134)$$

Let us note that we can also rewrite this result (actually one equivalent with the precision of our calculation) in terms of shape and jet functions as in Eq. (121). For the shape function, Eq. (122), we have to replace $m_Q \rightarrow m_{Q,R}$ and for the jet function, Eq. (118), we have to replace $m_c \rightarrow m_{c,R}$.

The expressions for the moments read

$$M_N^{pert} = \frac{G^2 M_{H_Q}}{4\pi} \frac{m_{Q,R}^2}{M_{H_Q}^2} \left(\frac{m_{Q,R}^2 - m_{c,R}^2}{m_{Q,R}^2}\right)^N \int_0^1 dx x^{N-2} \phi_{H_Q}^2(x). \quad (135)$$

This expression allows us to compare the hadronic and the effective field theory computations. It is quite remarkable that this result agrees with the hadronic result obtained in Eq. (83). Therefore, we also obtain the same expressions for M_N^{OPE} , Eq. (84), valid in the OPE kinematic region, and for M_N^{SCETI} , Eq. (85), valid in the SCETI kinematic region. The comments about the precision of the expressions made there also apply here. The expression for M_N^{OPE} is correct up to, and including, $O(1/m_Q^2)$ corrections. The expression for M_N^{SCETI} is correct up to, and including, $O(1/m_Q)$ corrections. The conclusion is

that, if working with moments, we do not see duality violations with the precision of our calculation.

It is interesting to compare with the computation of the moments made by Bigi et al. [4]. For the total decay width, M_1 , we obtain exactly the same analytic expression. Actually, this result is not affected by the radiative corrections (we obtain the same result at tree level or one-loop). In our opinion, this explains the agreement, since the computation of Bigi et al. has (effectively) been done at tree level. For $M_{0,2}$, we need to perform the one-loop computation in order to get agreement with their results with $O(1/m_Q^2)$ precision. This is quite remarkable, since in the kinematical situation they choose, $q^+ = 0$, it is argued that there is a non-renormalization theorem for the current, whereas in the kinematical situation $q^- = 0$ this is not true and the one-loop corrections to the vertex shown in Fig. 15 have to be included.

We are now in the position to perform a numerical analysis of the corresponding expressions obtained from effective field theories with perturbative factorization and to compare them with the hadronic ones. We first consider the differential decay rate. As we have already discussed throughout the paper, the direct comparison between the partonic and hadronic result is not possible since the first is an smooth function in x , whereas the second consists of a sum over deltas. Nevertheless, the layer-function approximation gives us a qualitative way to compare the hadronic matrix elements with the computation using the effective theory, since it allows us to write the hadronic matrix elements in terms of only the H_Q meson wave-function. Naively, one could make the following assignment to the hadronic matrix element from the effective field theory computation

$$\begin{aligned} & \pi\beta \frac{m_{Q,R}}{M_{H_Q}^2} \left(1 - \frac{m_{c,R}^2}{m_{Q,R}^2}\right) \frac{1}{x} \phi_{H_Q} \left(\frac{x}{1 - \frac{m_{c,R}^2}{m_{Q,R}^2}} \right) \\ & \simeq \pi\beta \frac{m_{Q,R}}{M_{H_Q}^2} \frac{1}{x} \phi_{H_Q}(x) \left[1 + 2x \frac{m_{c,R}^2}{M_{H_Q}^2} \left(\frac{\phi'_{H_Q}(x)}{\phi_{H_Q}(x)} - \frac{1}{2x} \right) \right], \end{aligned} \quad (136)$$

where the normalization has been adjusted to agree with the layer-function result. The LO result agrees with the LO layer-function expression, Eq. (66). Nevertheless, this is not so for the subleading one. We will elaborate on this issue at the end of this section. Although numerically the effect is not very important (we would obtain very similar plots to those obtained in Figs. 7 and 8), it is important from the conceptual point of view.

We now move to the comparison of the moments. In this case, the comparison is more sound. For all the numerical checks we have set $G^2/(4\pi) = 1$. We have compared the perturbative and hadronic result. The agreement is very good up to very high moments. We show this comparison in Fig. 16¹⁴. We also consider how convergent is the expansion either if we work in the strict OPE or SCETI regime. We show the convergence of the OPE expansion in Fig. 17. For the OPE limit we can see that the breakdown of the

¹⁴We also make the comparison for the set of masses used in Ref. [5], to illustrate how well our expressions would work for an hypothetical $b \rightarrow c\nu$ decay.

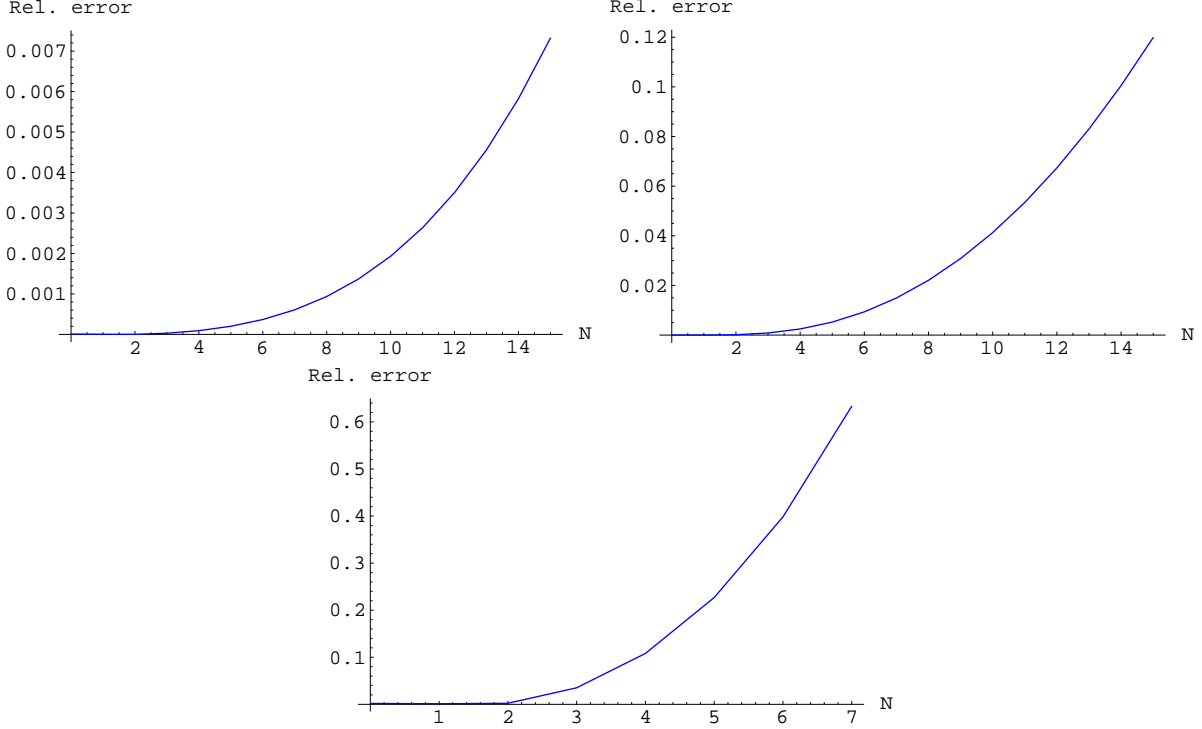


Figure 16: *Difference between the hadronic, Eq. (72), and perturbative, Eq. (135), result for the moments (divided by the hadronic result). The first figure is for the values $m_Q = 10\beta$, $m_c = \beta$ and $m_s = \beta$, the second is for the values $m_Q = 15\beta$, $m_c = 10\beta$ and $m_s = 0.56\beta$ and the third for the values $m_Q = 3\beta$, $m_c = \beta$ and $m_s = \beta$.*

agreement with the hadronic result appears earlier. This is to be expected since there is a new scale N/m_Q , which is not resummed. In any case the precision is better than 5% for N below 6 at NNLO. We also perform the analysis in the SCETI region. We show the plot in Fig. 18. As expected the convergence improves over the OPE evaluations and they are optimal for values of $N \sim m_Q/\beta$ as expected. For very large values of N , they blow up as expected. We also consider the dependence on the heavy quark mass of these results. For that we repeat the same analysis for $m_Q = 3$, which is somewhat the limiting case of validity of our results. Overall, we get a similar picture than before but with worse convergence (actually in the OPE region the results are barely convergent) and the perturbative results are only reliable for lower moments, again as expected. The effect of the one-loop corrections (the renormalization of the masses) is small.

Keeping the prefactor $\left(\frac{m_{Q,R}^2 - m_{c,R}^2}{m_{Q,R}^2}\right)^N$ improves the numerical agreement with the hadronic expression but we should remind that we cannot claim better accuracy than $\simeq 1 - N \frac{m_{c,R}^2}{m_{Q,R}^2}$. This effect is particularly important if the mass of the hard-collinear is large.

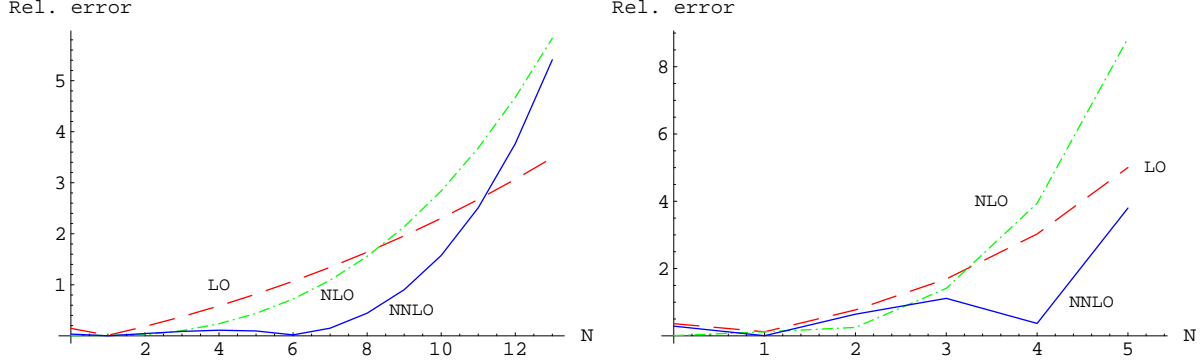


Figure 17: *Difference between the hadronic, Eq. (72), and perturbative, Eq. (84), result for the moments (divided by the hadronic result) in the OPE limit. The dashed line for the LO result, the dash-dotted line for the NLO result, and the solid line for the NNLO result. We take the values $m_Q = 10\beta$, $m_c = \beta$ and $m_s = \beta$ for the first figure and $m_Q = 3\beta$, $m_c = \beta$ and $m_s = \beta$ for the second figure. We use the values $\langle t \rangle = 1.73\beta$ and $\langle t^2 \rangle = 3.99\beta^2$, which can be checked with the sum rules of Ref. [23].*

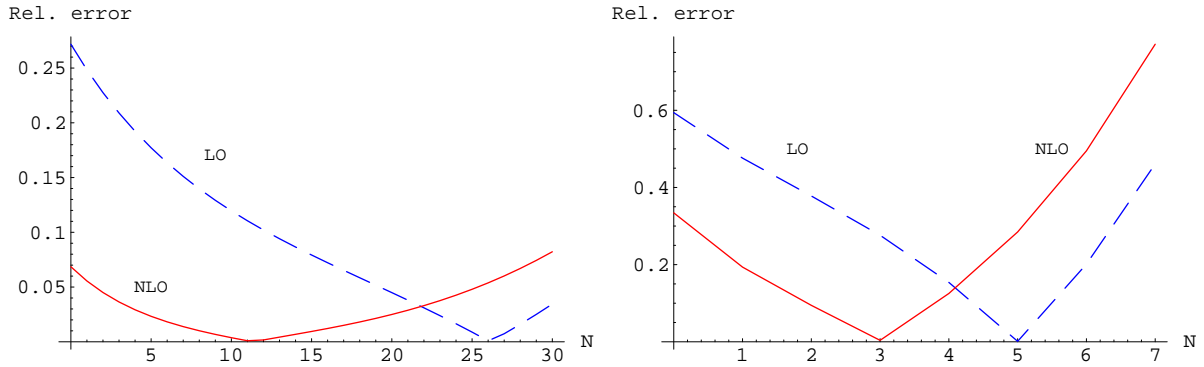


Figure 18: *Difference between the hadronic, Eq. (72), and perturbative, Eq. (85), result for the moments (divided by the hadronic result) in the SCET1 limit. The dashed line for the LO result, and the solid line for the NLO result. We take the values $m_Q = 10\beta$, $m_c = \beta$ and $m_s = \beta$ for the first figure and $m_Q = 3\beta$, $m_c = \beta$ and $m_s = \beta$ for the second figure.*

We now consider $\Gamma_{H_Q}(y)$. We compare the hadronic result versus the prediction from effective field theories in Fig. 19. We can see a good quantitative agreement between both lines but it is not possible to perform a point-to-point comparison because the hadronic result is a step-function whereas the perturbative computation is an smooth function in y . Therefore, it is difficult to quantify the error, which typically is of the order of the difference between the n and $n + 1$ state contribution to $\Gamma_{H_Q}(y)$.

To make more evident this problem, we now consider the average

$$\int_{x_n-\delta x}^{x_n+\delta x} \frac{d\Gamma}{dx} dx, \quad (137)$$

where δx is bounded to be small enough that only one resonance contributes to the integral. One could believe that the duality violations can be smoothed in this way. This definition provides the closest possible thing to a point-to-point comparison between the perturbative and hadronic result. Since we are now able to perform analytic computations both for the hadronic and for perturbative result, we are in the position to quantify this statement (we restrict to the kinematic regime where $M_n^2 \gg \beta^2$). We obtain the following result from the hadronic computation

$$\int_{x_n-\delta x}^{x_n+\delta x} \frac{d\Gamma}{dx} \Big|_{hadr.} dx = \Gamma_n \simeq \frac{\pi^2 \beta^2}{M_{H_Q}^2} \frac{G^2 M_{H_Q}}{4\pi} \frac{m_{Q,R}^2}{M_{H_Q}^2} \frac{1}{x_n} \phi_{H_Q}^2(x_n) \left[1 + 2 \frac{m_{c,R}^2}{M_{H_Q}^2} \left(\frac{\phi'_{H_Q}(x_n)}{\phi_{H_Q}(x_n)} - \frac{1}{x_n} \right) \right]. \quad (138)$$

From the perturbative computation we obtain

$$\int_{x_n-\delta x}^{x_n+\delta x} \frac{d\Gamma}{dx} \Big|_{pert.} dx \simeq 2\delta x \frac{G^2 M_{H_Q}}{4\pi} \frac{m_{Q,R}^2}{M_{H_Q}^2} \frac{1}{x_n} \phi_{H_Q}^2(x_n) \left[1 + 2x_n \frac{m_{c,R}^2}{M_{H_Q}^2} \left(\frac{\phi'_{H_Q}(x_n)}{\phi_{H_Q}(x_n)} - \frac{1}{2x_n} \right) \right]. \quad (139)$$

We can see that both expressions are different, even at leading order, due to the normalization. Only if we fine tune δx to a very specific value (actually, the one chosen in Ref. [5]), we get agreement between both expressions, and, even then, the subleading corrections are different¹⁵. In order to fine tune the value of δx , we should have a good knowledge of the non-perturbative spectrum (this is certainly difficult in the four-dimension case, although one can always assume a linear regge behavior), which is something that we do not expect can be achieved from perturbation theory. On the other hand, as far as δx is independent of n , one obtains this equality at leading order (subleading corrections remain to be different)

$$\frac{\int_{x_{n+1}-\delta x}^{x_{n+1}+\delta x} \frac{d\Gamma}{dx} \Big|_{hadr.} dx}{\int_{x_n-\delta x}^{x_n+\delta x} \frac{d\Gamma}{dx} \Big|_{hadr.} dx} = \frac{\int_{x_{n+1}-\delta x}^{x_{n+1}+\delta x} \frac{d\Gamma}{dx} \Big|_{pert.} dx}{\int_{x_n-\delta x}^{x_n+\delta x} \frac{d\Gamma}{dx} \Big|_{pert.} dx} \quad (140)$$

without fine-tuning δx .

¹⁵Actually, these small differences for the subleading corrections are crucial to get agreement for the moments at $O(1/m_Q^2)$.

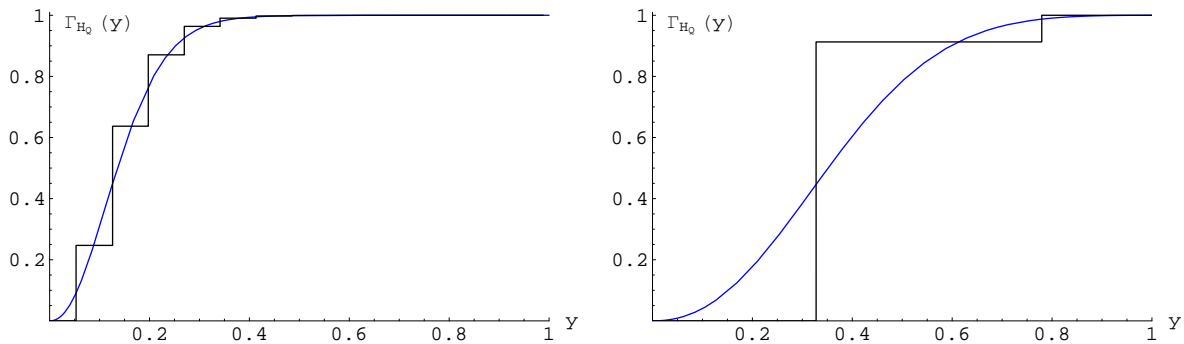


Figure 19: Plot of $\Gamma_{H_Q}(y)$ using the hadronic or perturbative expression of $d\Gamma/dx$. The smooth curve represents the perturbative prediction and the other line is the hadronic one. We take the values $m_Q = 10\beta$, $m_c = \beta$ and $m_s = \beta$ for the first figure and $m_Q = 3\beta$, $m_c = \beta$ and $m_s = \beta$ for the second figure.

6 Conclusions

We have studied QCD in 1+1 dimensions in the large N_c limit using light-front Hamiltonian perturbation theory in the $1/N_c$ expansion. We have used the formalism developed to exactly compute hadronic transition matrix elements for arbitrary currents at leading order in $1/N_c$. We have compared with previous results found in the literature. We have computed in two alternative ways the semileptonic differential decay rate of a heavy meson and its moments using the previously computed hadronic matrix elements. They yield very different expressions for the differential decay rate, which should be equal by parity invariance. This has led to the derivation of non-trivial equalities between matrix elements, which we have checked numerically. Some partial analytic checks have also been done.

We have then focused on the kinematic regime where the OPE ($N \sim x \sim 1$) or SCETI ($1 - x \sim 1/N \sim \beta/m_Q$) can be applied. This means $n \gg 1$, where n is the principal quantum number of the final hadronic state. This has allowed us to use the properties of the final hadronic bound state in those kinematical regimes by using the layer function [7,18]. The resulting expressions are suitable to a more direct connection with the computation obtained using perturbative factorization. We have then obtained expressions for the moments using the EulerMcLaurin formula, within an expansion in $1/m_Q$, either in the OPE or in the SCETI regions. In the first case up to order $1/m_Q^2$ and in the second up to order $1/m_Q$. We have also checked that these results agree with the expressions of the sum rules for $N = 0, 1, 2$ obtained in Ref. [4] up to order $1/m_Q^2$ (we have also checked them by direct computation).

We have also studied the differential decay rate using effective theories with perturbative factorization. We have first derived SCETI at leading order in 1+1 dimensions, and applied it to the differential decay rate. We have seen that there is a strong simplification

working in the light-cone quantization frame, which allows us to relate the shape function with the wave-function of the bound state (in the large N_c). We have then dwelt further on the issue of finding the optimal effective theory to describe the differential decay rate in the OPE and SCETI kinematical regime. We see that, at least in two dimensions, it appears to be more efficient to integrate out the hard-collinear modes and only keep soft degrees of freedom. This takes advantage of the fact that the hard-collinear interactions only appear in a very specific way, emanating from the weak interaction, whereas in the standard construction of SCETI one works out all possible couplings. The resulting effective theory is equal to HQET plus some imaginary terms, which describe the differential decay rate. This effective theory is more efficiently implemented in the light-front quantization frame, where it becomes "local" in the " x^+ " quantization frame, and it is suitable for computations in a Hamiltonian formulation. We have then obtained the differential decay rate at one-loop. We would also like to remark that some of these ideas could also apply to the four-dimensional case, where it also seems possible to obtain a "local" effective interaction in the " x^+ " quantization frame.

At the end of the day, we have been able to obtain expressions for the moments using effective field theories with perturbative factorization with relative accuracy of $O(\beta^2/m_Q^2)$ in the kinematical regime where the OPE can be applied, and with relative accuracy of $O(\beta/m_Q)$ in the kinematical regime where non-local effective field theories can be applied. These expressions agree, within this precision, with those obtained from the hadronic expressions using the layer-function approximation plus Euler-McLaurin expansion (taking into account the numerical agreement for the radiative correction).

Numerically very good agreement for the moments between the exact result and the result using effective field theories with perturbative factorization is obtained. For the differential decay rate it is also possible to perform a sort of comparison between the hadronic and perturbative result based on the layer-function approximation. The agreement is very good if we do not approach too much the limit $x \rightarrow 1$.

There is still the issue of the theoretical error. As we have mentioned throughout the paper, it is not possible to make a quantitative comparison (with errors) between the hadronic and perturbative differential decay rate, since one is represented by a sum of deltas whereas the other is a smooth function in x . Therefore, effective field theories with perturbative factorization are not suitable to predict the differential decay rate on a point-to-point basis. Note that this comment also applies to $\Gamma_{H_Q}(y)$ and, in principle, to other arbitrarily smeared functions. This is best illustrated in the derivation of SCETI at leading order where, after field redefinitions, one is led to an effective theory where the hard-collinear is a free field. Therefore, it can never build a bound state, which is what is observed in the hadronic differential decay rate. Effective field theories with perturbative factorization can only hopefully be a good approximation (or at least a good starting point) for inclusive observables on which one averages over a large fraction of the final bound states (this is a handicap from the experimental point of view, since one has to know the differential decay rate for arbitrarily large momenta). This motivates the use of moments¹⁶ for the comparison, since they may lead to a "quantitative" comparison

¹⁶When we perform the comparison among moments the difference is "less severe" than using directly

between hadronic and perturbative results. With the precision obtained in this paper we obtain a perfect match between the hadronic and perturbative results. Nevertheless, to have a more rigorous handle of the errors, one should be able to quantify the error produced by using the layer-function (i.e. to consider subleading effects in the WKB approximation), as well as by using the Euler-McLaurin formula. Actually it is this last formula that allows to make quantitative the comparison of perturbative and non-perturbative results. We expect to come back to these issues in the future in order to try to find duality violations in the computation of the moments in the SCETI kinematical region.

Acknowledgments:

The work of J.M. and A.P. was supported in part by a *Distinció* from the *Generalitat de Catalunya*, as well as by the contracts MEC FPA2004-04582-C02-01, CIRIT 2005SGR-00564 and the EU network EURIDICE, HPRN-CT2002-00311. The work of J.R. was supported in part by the contract MEC FPA2002-2415.

A Conventions and notation

In this appendix the conventions and notation that we use are presented. We define two light-like vectors (with the metric $g^{+-} = g^{-+} = 2$ and zero elsewhere),

$$n_-^\mu = (1, 1), \quad n_+^\mu = (1, -1), \quad (141)$$

where light-cone coordinates are defined in the usual way,

$$x^+ \equiv n_+ \cdot x = (x^0 + x^1), \quad x^- \equiv n_- \cdot x = (x^0 - x^1), \quad (142)$$

which imply that

$$x^0 \equiv \frac{1}{2}(x^+ + x^-), \quad x^1 \equiv \frac{1}{2}(x^+ - x^-), \quad (143)$$

and

$$\partial^- = 2 \frac{\partial}{\partial x^+} = \frac{\partial}{\partial x^0} + \frac{\partial}{\partial x^1} = \partial_0 + \partial_1 \sim p^-, \quad \partial^+ = 2 \frac{\partial}{\partial x^-} = \frac{\partial}{\partial x^0} - \frac{\partial}{\partial x^1} = \partial_0 - \partial_1 \sim p^+, \quad (144)$$

$$P \cdot x = \frac{P^+ x^-}{2} + \frac{P^- x^+}{2}, \quad (145)$$

$$d^D x = \frac{1}{2} dx^+ dx^- d^{D-2} x_\perp. \quad (146)$$

the differential decay rate. The point is to quantify the "less severe" at the parametrical level (although it can be done at the numerical level). For the moments $N = 0, 1, 2$, this has already been done in Ref. [4].

For the Dirac algebra is useful to define the corresponding light-cone matrices

$$\not{n}_+ = \gamma^+, \quad \not{n}_- = \gamma^-. \quad (147)$$

To have explicit expressions, it is useful to work with an explicit representation of the Dirac algebra. We will use the following Weyl-like representation for the Dirac algebra

$$\gamma^0 = \begin{pmatrix} 0 & -i \\ i & 0 \end{pmatrix} \quad \gamma^1 = \begin{pmatrix} 0 & i \\ i & 0 \end{pmatrix}, \quad (148)$$

so that the corresponding light cone matrices are given by

$$\gamma^- = -2i \begin{pmatrix} 0 & 1 \\ 0 & 0 \end{pmatrix} \quad \gamma^+ = 2i \begin{pmatrix} 0 & 0 \\ 1 & 0 \end{pmatrix}. \quad (149)$$

This way one can see the explicit effect of the projection operators ($\gamma_5 = \gamma^0\gamma^1$)

$$\begin{aligned} \Lambda_+ &\equiv \frac{1 + \gamma_5}{2} = \frac{\gamma^0\gamma^+}{2} = \frac{1}{4}\not{n}_-\not{n}_+ = \frac{1}{4}\gamma^-\gamma^+ = \begin{pmatrix} 1 & 0 \\ 0 & 0 \end{pmatrix}, \\ \Lambda_- &\equiv \frac{1 - \gamma_5}{2} = \frac{\gamma^0\gamma^-}{2} = \frac{1}{4}\not{n}_+\not{n}_- = \frac{1}{4}\gamma^+\gamma^- = \begin{pmatrix} 0 & 0 \\ 0 & 1 \end{pmatrix}, \end{aligned} \quad (150)$$

in the sense that if one splits a quark doublet on its two components

$$\psi = \begin{pmatrix} \psi_+ \\ \psi_- \end{pmatrix}, \quad (151)$$

then the projection operators act as expected

$$\Lambda_+\psi = \begin{pmatrix} \psi_+ \\ 0 \end{pmatrix} \quad \Lambda_-\psi = \begin{pmatrix} 0 \\ \psi_- \end{pmatrix}. \quad (152)$$

References

- [1] M. A. Shifman, arXiv:hep-ph/0009131.
- [2] G. 't Hooft, Nucl. Phys. B **72**, 461 (1974).
- [3] G. 't Hooft, Nucl. Phys. B **75**, 461 (1974).
- [4] I. I. Y. Bigi, M. A. Shifman, N. Uraltsev and A. I. Vainshtein, Phys. Rev. D **59**, 054011 (1999) [arXiv:hep-ph/9805241].
- [5] R. F. Lebed and N. G. Uraltsev, Phys. Rev. D **62**, 094011 (2000) [arXiv:hep-ph/0006346].
- [6] C. G. Callan, N. Coote and D. J. Gross, Phys. Rev. D **13**, 1649 (1976).

- [7] M. B. Einhorn, Phys. Rev. D **14**, 3451 (1976).
- [8] C. W. Bauer, S. Fleming and M. E. Luke, Phys. Rev. D **63**, 014006 (2001) [arXiv:hep-ph/0005275].
- [9] C. W. Bauer, S. Fleming, D. Pirjol and I. W. Stewart, Phys. Rev. D **63**, 114020 (2001) [arXiv:hep-ph/0011336].
- [10] C. W. Bauer, D. Pirjol and I. W. Stewart, Phys. Rev. D **65**, 054022 (2002) [arXiv:hep-ph/0109045].
- [11] M. Beneke, A. P. Chapovsky, M. Diehl and T. Feldmann, Nucl. Phys. B **643**, 431 (2002) [arXiv:hep-ph/0206152].
- [12] T. Becher, R. J. Hill and M. Neubert, Phys. Rev. D **69**, 054017 (2004) [arXiv:hep-ph/0308122].
- [13] C. W. Bauer, M. P. Dorsten and M. P. Salem, Phys. Rev. D **69**, 114011 (2004) [arXiv:hep-ph/0312302].
- [14] A. V. Manohar and I. W. Stewart, arXiv:hep-ph/0605001.
- [15] P. A. M. Dirac, Rev. Mod. Phys. **21**, 392 (1949).
- [16] P. Gaete, J. Gamboa and I. Schmidt, Phys. Rev. D **49**, 5621 (1994) [arXiv:hep-th/9311066].
- [17] N. Brambilla, A. Pineda, J. Soto and A. Vairo, Rev. Mod. Phys. **77**, 1423 (2005) [arXiv:hep-ph/0410047].
- [18] R. C. Brower, W. L. Spence and J. H. Weis, Phys. Rev. D **19**, 3024 (1979).
- [19] M. Burkardt and E. S. Swanson, Phys. Rev. D **46**, 5083 (1992).
- [20] B. Grinstein and R. F. Lebed, Phys. Rev. D **57**, 1366 (1998) [arXiv:hep-ph/9708396].
- [21] J. L. F. Barbon and K. Demeterfi, Nucl. Phys. B **434**, 109 (1995) [arXiv:hep-th/9406046].
- [22] M. Burkardt, Nucl. Phys. A **504**, 762 (1989).
- [23] M. Burkardt and N. Uraltsev, Phys. Rev. D **63**, 014004 (2001) [arXiv:hep-ph/0005278].
- [24] M. Beneke and V. A. Smirnov, Nucl. Phys. B **522**, 321 (1998) [arXiv:hep-ph/9711391].
- [25] M. Beneke, F. Campanario, T. Mannel and B. D. Pecjak, JHEP **0506**, 071 (2005) [arXiv:hep-ph/0411395].

- [26] C. W. Bauer, D. Pirjol and I. W. Stewart, Phys. Rev. D **67**, 071502 (2003) [arXiv:hep-ph/0211069].
- [27] J. Rojo, arXiv:hep-ph/0601229.